

PREFACE

International Energy Agency

The International Energy Agency (IEA) was established in 1974 within the framework of the Organization for Economic Co-operation and Development (OECD) to implement an International Energy Programme. A basic aim of the IEA is to foster co-operation among the twenty-one IEA Participating Countries to increase energy security through energy conservation, development of alternative energy sources and energy research development and demonstration (RD&D). This is achieved in part through a programme of collaborative RD&D consisting of forty-two Implementing Agreements, containing a total of over eighty separate energy RD&D projects. This publication forms one element of this programme.

Energy Conservation in Buildings and Community Systems Programme

The IEA sponsors research and development in a number of areas related to energy. In one of these areas, Energy Conservation in Buildings and Community Systems (BCS), the IEA is sponsoring various exercises to predict more accurately the energy use of buildings, including comparison of existing computer programs, building monitoring, comparison of calculation methods, as well as air quality and studies of occupancy. Seventeen countries have elected to participate in this area and have designated contracting parties to the Implementing Agreement covering collaborative research in this area. The designation by governments of a number of private organizations, as well as universities and government laboratories, as contracting parties, has provided a broader range of expertise to tackle the projects in the different technology areas than would have been the case if participation was restricted to governments. The importance of associating industry with government sponsored energy research and development is recognized in the IEA, and every effort is made to encourage this trend.

Overall control of the programme is maintained by an Executive Committee, which not only monitors existing projects but identifies new areas where collaborative effort may be beneficial. The Executive Committee ensures that all projects fit into a pre-determined strategy, without unnecessary overlap or duplication but with effective liaison and communication. The Executive Committee has initiated the following projects to date (completed projects are identified by *).

- Annex 1: Load energy determination of buildings *
- Annex 2: Ecistics & advanced community energy systems *
- Annex 3: Energy conservation in residential buildings *
- Annex 4: Glasgow commercial building monitoring *
- Annex 5: Air infiltration and ventilation centre
- Annex 6: Energy systems and design of communities *
- Annex 7: Local government energy planning *
- Annex 8: Inhabitants behaviour with regard to ventilation *
- Annex 9: Minimum ventilation rates *
- Annex 10: Building HVAC system simulation *
- Annex 11: Energy auditing *
- Annex 12: Windows and fenestration *
- Annex 13: Energy management in hospitals *
- Annex 14: Condensation and energy *
- Annex 15: Energy efficiency of schools *
- Annex 16: BEMS 1 - User interfaces and system integration
- Annex 17: BEMS 2 - Evaluation and emulation techniques
- Annex 18: Demand controlled ventilating systems
- Annex 19: Low slope roofs systems
- Annex 20: Air flow patterns within buildings
- Annex 21: Calculation of energy & environmental performance of buildings
- Annex 22: Energy efficient communities
- Annex 23: Multizone air flow modelling
- Annex 24: Heat, air & moisture transport in new and retrofitted insulated envelope parts

(ii)

- Annex 25: Real time simulation of HVAC systems and fault detection
- Annex 26: Energy-efficient ventilation of large enclosures
- Annex 27: Evaluation and demonstration of domestic ventilation systems
- Annex 28: Low-energy cooling systems

Annex 21: Calculation of Energy and Environmental Performance of Buildings

The objectives of Annex 21 are to:

- 1) develop quality assurance procedures for calculating the energy and environmental performance of buildings by producing guidance on:
 - program and modelling assumptions
 - the appropriate use of calculation methods for a range of design applications
 - the evaluation of calculation methods
- 2) establish requirements and market needs for calculation procedures in building and environmental services design;
- 3) propose policy and strategic direction for the development of calculation procedures;
- 4) propose means to effect technology transfer of calculation procedures into the building and environmental services design profession.

The subtasks of this project are:

- A. Documentation of Existing Methods
- B. The Appropriate Use of Models
- C. Reference Cases and Evaluation Procedures
- D. Design Support Environment

The participants in this annex are: Belgium, France, Germany, Italy, the Netherlands, Switzerland and the United Kingdom. Canada, Finland and Sweden also participated in the early part of the project. In addition, Finland, Spain, Sweden and the United States participate in Subtask C as a collaborative research activity between Task 12 Subtask B of the IEA Solar Heating & Cooling Programme.

The UK Building Research Establishment acts as Operating Agent of BCS Annex 21.

Solar Heating and Cooling Programme

Initiated in 1977, the Solar Heating and Cooling (SHC) Programme was one of the first IEA R&D agreements. Its objective is to conduct joint projects between the 20 member countries to advance solar technologies for buildings.

A total of eighteen projects or "Tasks" have been undertaken since the beginning of the Programme. The overall programme is managed by an Executive Committee composed of one representative from each of the member countries, while the leadership and management of the individual Tasks is the responsibility of Operating Agents. These Tasks and their respective Operating Agents are (completed projects are identified by *, tasks in planning stage are identified by #):

- Task 1: Investigation of the performance of solar heating and cooling systems - Denmark *
- Task 2: Co-ordination of research and development on solar heating and cooling - Japan *
- Task 3: Performance testing of solar collectors - United Kingdom *
- Task 4: Development of an insulation handbook and instrument package - United States *
- Task 5: Use of existing meteorological information for solar energy application - Sweden *
- Task 6: Solar heating, cooling, and hot water systems using evacuated collectors - United States *
- Task 7: Central solar heating plants with seasonal storage - Sweden *
- Task 8: Passive and hybrid solar low energy buildings - United States *
- Task 9: Solar radiation and pyranometry studies - Germany *
- Task 10: Material research and testing - Japan *
- Task 11: Passive and hybrid solar commercial buildings - Switzerland *

(iii)

- Task 12: Building energy analysis and design tools for solar applications - United States
- Task 13: Advanced solar low energy buildings - Norway
- Task 14: Advanced active solar systems - Canada
- Task 15: Advanced central solar heating plants #
- Task 16: Photovoltaics in buildings - Germany
- Task 17: Measuring and modelling spectral radiation - Germany
- Task 18: Advanced glazing materials - United Kingdom
- Task 19: Solar air systems - Switzerland
- Task 20: Solar retrofit systems - Sweden

Task 12: Building Energy Analysis and Design Tools for Solar Applications

The scope of Task 12 includes:

- (1) selection and development of appropriate algorithms for modelling of the interaction of solar energy-related materials, components, and systems with the building in which these solar elements are integrated;
- (2) selection of analysis and design tools, and evaluation of the algorithms as to their ability to model the dynamic performance of the solar elements in respect of accuracy and ease of use; and
- (3) improvement of the usability of the analysis and design tools, through preparation of common formats and procedures and by standardization of specifications for input/output, default values, and other user-related factors.

The subtasks of this project are:

- A) Model Development
- B) Model Evaluation and Improvement
- C) Model Use

The participants in this task are: Denmark, Finland, Germany, Norway, Spain, Sweden, Switzerland, and the United States. In addition, Belgium, France, Italy, and the United Kingdom participate in Subtask B as a collaborative research activity between Annex 21 Subtask C of the IEA Energy Conservation in Building and Community Systems Program.

Architectural Energy Corporation serves on behalf of the US Department of Energy as Operating Agent of SHC Task 12.

ACKNOWLEDGEMENTS

The authors are grateful to the UK Building Research Establishment for funding this work. We wish to thank the joint TEA BCS Annex 21, Subtask C and SHC Task 12, Subtask B members for their valuable contributions and support:

Viottorio Bocchio / Augusto Mazza, Politecnico di Torino, Italy (BLASTv3.0);
Pascal Dalicieux, EDF, France (CLIM2000v1.1);
Tapio Haapala / Timo Kalema, Tampere University of Technology, Finland (TASEv3.0);
Shirley Hammond, BRE (SERI-RESv1.2);
Foroutan Parand, BRE (TRNSYSv12.1 & 13.1);
Eduardo Rodriguez, Escuela Superiore Ingnieros Industriales, Seville, Spain (S3PASv2.0);
Peter Verstraete / Rik van de Perre, Vrije Universiteit Brussel, Belgium (TRNSYSv13.1);
Ron Judkoff, NREL, Chair of IEA BCS 21C / SHC 12B experts group
Michael Holtz, Architectural Energy Corporation

We are also indebted to all those who participated, without any dedicated funding, by running their thermal programs. Without these contributions the work would have been far less comprehensive:

Lorenzo Agnoletto, Instituto di Fisica Technica, Udine, Italy (WG6TCv1992);
Don Alexander, UWCC Cardiff (HTB2v1.10);
Angelo Delsante, CSIRO, Australia (CHEETAHv1.2);
Martin Gough / Alan Jones, EDSL (TASv7.54);
Mike Holmes, Arup R&D (ENERGY2v1.0);
Kjeld Johnsen, SBI, Denmark (TSBI3v2.0);
Mike Kennedy, ECOTOPE, USA (SUNCODEv5.7);
Brian Miller / Doug Hittle, Colorado State University, USA (BLASTv3.0);
Peter Moors, DMU (TASv7.54);
Peter Pfrommer, FHT Stuttgart, Germany (HTB2v1.2);
Paul Strachan, ESRU (ESP-rv7.7a);
Glenn Stuart, ASL Sterling (ESP+v2.1);
Andrew Tindale, FACET (3TCv1.0 & APACHEv6.5.3);
Jeff Thornton, University of Wisconsin, USA (TRNSYSv13.1);
Maria Wall / Petter Wallenten, Lund University, Sweden (DEROBv1th);
Fred Winkelmann, LBL, USA (DOE2v1E).

The permission of the UK Energy Technology Support Unit to use the data from the Energy Monitoring Company test rooms is gratefully acknowledged.

Overview

This report describes part of the empirical validation work undertaken under the auspices of the group formed by combining International Energy Agency (IEA) Building and Community Systems (BCS) Annex 21 Subtask C and IEA Solar Heating and Cooling (SHC) Task 12 Subtask B.

The work was directed by the UK Building Research Establishment (BRE), and managed by the Environmental Computer Aided Design and Performance (ECADAP) group in the School of the Built Environment at De Montfort University Leicester, and by the Energy Monitoring Company (EMC), Newport Pagnell, UK. The latter two participated via sub-contracts from the BRE.

This report is part of a 3 volume set, produced by the UK participants:

- Volume 1: Final Report
- Volume 2: Empirical Validation Package
- Volume 3: Working Reports

This empirical validation work complements the work using other evaluation techniques undertaken within the IEA BCS Annex 21/ SHC Task 12 group. These activities resulted in the production of a set of Building Energy Simulation Tests (BESTESTs), based on inter-model comparisons. These tests, based on domestic scale buildings, are structured such that reasons for a program not properly predicting a building's performance can be diagnosed. Other tests based on intermodel comparisons relate to commercial buildings. Some work was also undertaken to develop analytic tests.

The Empirical Validation Package

This Validation Package is an updated collection of reports which were used in International Energy Agency (IEA) Annex 21 / Task 12 between March 1992 and September 1993 to evaluate the predictions from over 25 combinations of detailed thermal simulation program and user.

The Package has 4 parts:

- Part 1: Site Handbook
- Part 2: Validation Guidebook
- Part 3: Quality Assurance Report
- Part 4: Data Disk

CONTENTS

	page
1 INTRODUCTION	1
2 GENERAL DESCRIPTION OF THE TEST FACILITY	1
3 LOCATION AND SITE TOPOGRAPHY	2
4 TEST ROOM GEOMETRY	2
5 TEST ROOM CONSTRUCTION AND OPERATION	2
5.1 Test room construction details	3
5.2 Roofspace construction description	6
5.3 Distribution of solar radiation within the test rooms	8
5.4 Infiltration	8
5.5 Heat source characteristics	9
6 DATA ACQUISITION SYSTEM	9
6.1 Timing of recorded data	10
6.2 Sensor types, locations and accuracies	10
6.3 Data processing	11
7 DATA SETS	12
7.1 Data set periods	12
7.2 Climate summaries for data sets	12
7.3 Test room operation	13
7.4 Meteorological data file format	13
8 SENSITIVITY ANALYSIS	14
8.1 Notes about Parameter Uncertainties	16
8.2 Further Comments on Parameter Uncertainty	18

REFERENCES

FIGURES

APPENDIX 1 - Calculation of corrections for thermal edge effects

APPENDIX 2 - Distribution of solar radiation entering glazed test rooms

APPENDIX 3 - Timing of weather data supplied

LIST OF FIGURES

- Figure 3.1: Plan of test site
- Figure 4.1: Test building internal geometry
- Figure 5.1: Plan view of test room showing construction
- Figure 5.2: Section of test room on XX showing construction
- Figure 5.3: Section of test room on YY showing construction
- Figure 5.4: Layout of recommended test room surface constructions
- Figure 5.5: Layout of recommended roofspace surface constructions
- Figure 7.1: Volume 099: Air temperature and relative humidity
- Figure 7.2: Volume 099: Global and diffuse horizontal solar radiation
- Figure 7.3: Volume 099: Wind speed and direction
- Figure 7.4: Volume 110: Air temperature
- Figure 7.5: Volume 110: Global and diffuse horizontal solar radiation
- Figure 7.6: Volume 110: Wind speed and direction

LIST OF TABLES

	page
Table 3.1: Site details	2
Table 5.1: Test room surface finishes	3
Table 5.2: Test room floor construction	3
Table 5.3: Test room North wall construction	4
Table 5.4: Test room East wall construction	4
Table 5.5: Test room South wall construction	5
Table 5.6: Test room West wall construction	5
Table 5.7: Test room Ceiling construction	6
Table 5.8: Test room alternative South facing glazing options	6
Table 5.9: Transmission properties of glass	6
Table 5.10: Roofspace surface finishes	7
Table 5.11: Roofspace Floor construction	7
Table 5.12: Roofspace North wall construction	7
Table 5.13: Roofspace East wall construction	7
Table 5.14: Roofspace South wall construction	8
Table 5.15: Roofspace West wall construction	8
Table 5.16: Roof construction	8
Table 5.17: Test room heater characteristics	9
Table 6.1: Sensor descriptions and accuracies	11
Table 7.1: Data set start and finish dates	12
Table 7.2: Mean values of measured climate variables over experimental periods	13
Table 7.3: Test room heater operation	13
Table 7.4: Meteorological data file formats	14
Table 8.1: Uncertainty in the parameters supplied in the Site Handbook	15

1 INTRODUCTION

This document contains all the data required to model the Energy Monitoring Company (EMC) Outdoor Test Rooms using detailed thermal programs of buildings. It aims to describe the rooms in a similar level of detail as would be available when programs are used to address real design problems. The accompanying data diskette (Part 4) contains meteorological data from two ten day experiments during which three highly monitored test rooms were equipped with single glazing, double glazing and an opaque infill panel. During the first experiment the test rooms were unheated, and the second features heated operation to a fixed setpoint for part of the day. The simulations which may be carried out with the data are described in full in Part 2 of the Validation Package, the Validation Guidebook.

Part 3, the Quality Assurance Report, describes the effort to ensure that this validation package is of the highest possible quality.

This document was first produced for the work in International Energy Agency Annex 21C/ Task 12B between March 1992 and September 1993, in which 25 different combinations of program and user were evaluated.

Section 2 of this Site Handbook contains a short description of the test site. Section 3 describes the location and layout of the site in detail. Section 4 gives details of the physical construction of the test rooms, and Section 5 contains the suggested way of entering that construction into thermal simulation models, and also gives full details of the glazing options employed and performance of the heat source. Section 6 describes the instrumentation used in the test rooms. Finally, Section 7 describes the operation of the test rooms over the two experimental periods for which meteorological data has been supplied, summarises that data and describes the format in which it is supplied.

2 GENERAL DESCRIPTION OF THE TEST FACILITY

The EMC Outdoor Test Facility was established in April 1985. Initially it consisted of eight test rooms, in four semi-detached pairs. A ninth room was constructed on the site in 1986, and a tenth in 1992.

Since its inception the site has been used to carry out experiments for a wide range of clients, including the UK Department of Energy (the work being managed by the Energy Technology Support Unit, or ETSU), the British Gas Corporation (later British Gas plc), and the Rutherford Appleton Laboratory (UK Science and Engineering Research Council). The work carried out has fallen under three main headings:

- component testing, in which the performance of specific building elements has been determined. The most recent of these tests was of a wall clad with Transparent Insulation Material (TIM),
- investigation of the physical processes which underlie the thermal performance of buildings, for example the interaction of solar radiation with building fabric, and convective heat transfer processes, and
- empirical model validation studies, in which data from the test rooms is compared with predictions of their performance from a simulation model.

The data sets supplied with this document are from experiments conducted in three of the eight semi-detached rooms. These rooms are of lightweight, timber framed, construction. Thermal mass in the rooms is provided by the plasterboard lining of the walls and ceiling, and by a concrete slab floor. They are not unrepresentative of current UK timber framed housing.

These rooms feature interchangeable glazing panels in their south walls. These allow different glazing options to be quickly installed in the test rooms. The data sets described in this report were gathered from rooms with single glazing, double glazing and no glazing at all.

3 LOCATION AND SITE TOPOGRAPHY

The test site is located on the edge of Cranfield airfield in Bedfordshire, approximately 70 km North-west of London.

The site is at latitude 52.07°N and longitude 0.63°W, approximately 100 m above mean sea level. It can be located on UK Ordnance Survey Landranger sheet 153 at grid reference SP 937 420. The site is in a rural location, with an unobstructed view to the south over the airfield, which is estimated to have a ground reflectivity of 0.2.

Figure 3.1 shows the layout of the test buildings on the site. The glazed surfaces of the buildings face 9° West of South. In the following text this surface will be referred to as the South wall of the test rooms, with the other walls named accordingly.

Table 3.1 summarises the details of the site.

Latitude	52.07°N
Longitude	0.63°W
Altitude	100 m above msl
Exposure	Rural isolated
Ground reflectivity	0.2
Glazing orientation	9° West of South

Table 3.1: Site details

4 TEST ROOM GEOMETRY

As described in Section 2 the test rooms are in handed pairs. The distance between each pair is 0.9m (Figure 3.1). The internal geometry of a pair of rooms and their associated roofspaces is shown in Figure 4.1.

The window units in the glazed cells are mounted close to the front surface of the cell, to minimise shading effects. The front surface of the glazing is set 10 mm back from the front of the window frame.

The test rooms are supported approximately 300 mm above the ground, with free air circulating beneath them. It is therefore not necessary to model heat loss to the ground in order to predict their performance.

5 TEST ROOM CONSTRUCTION AND OPERATION

Figures 5.1 to 5.3 show the physical construction of the test rooms. These figures actually show the construction of Rooms 0, 2 and 4. The rooms used in this exercise are 1, 3 and 5, which are exact mirror images of the room shown. Figure 5.4 shows the layout of surface constructions which is

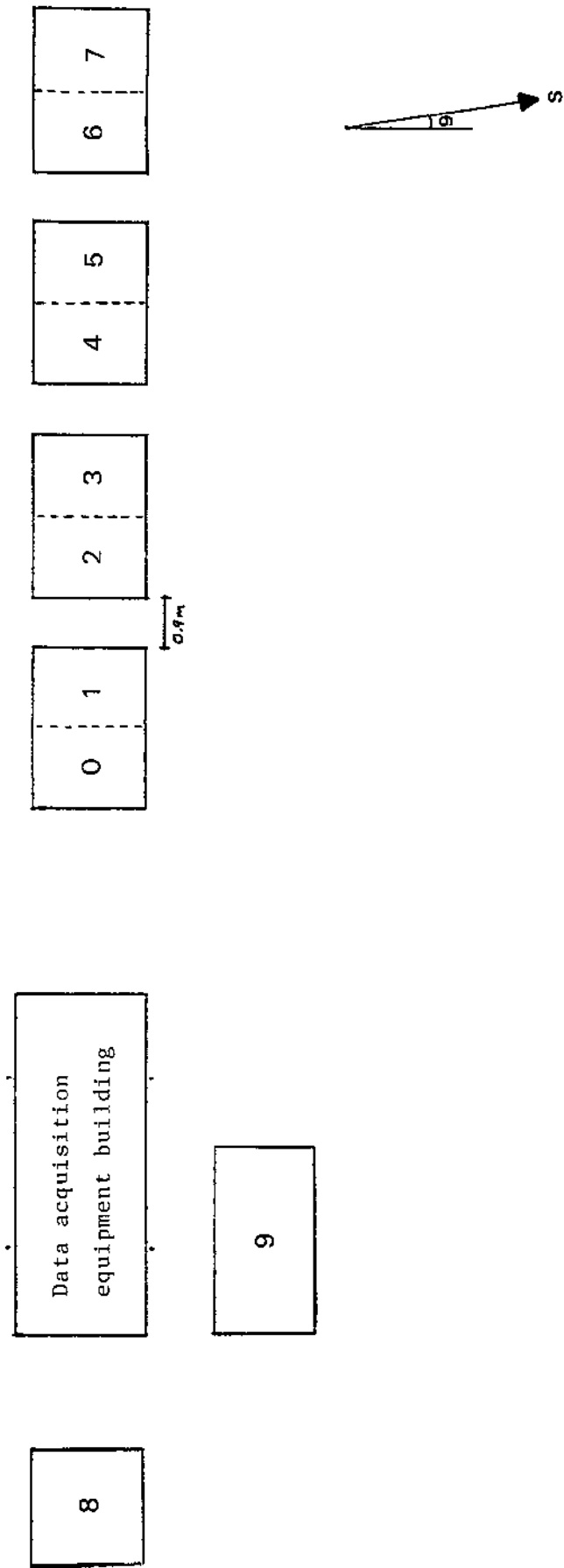


Figure 3.1: Plan of test site (scale approximately 1:40)

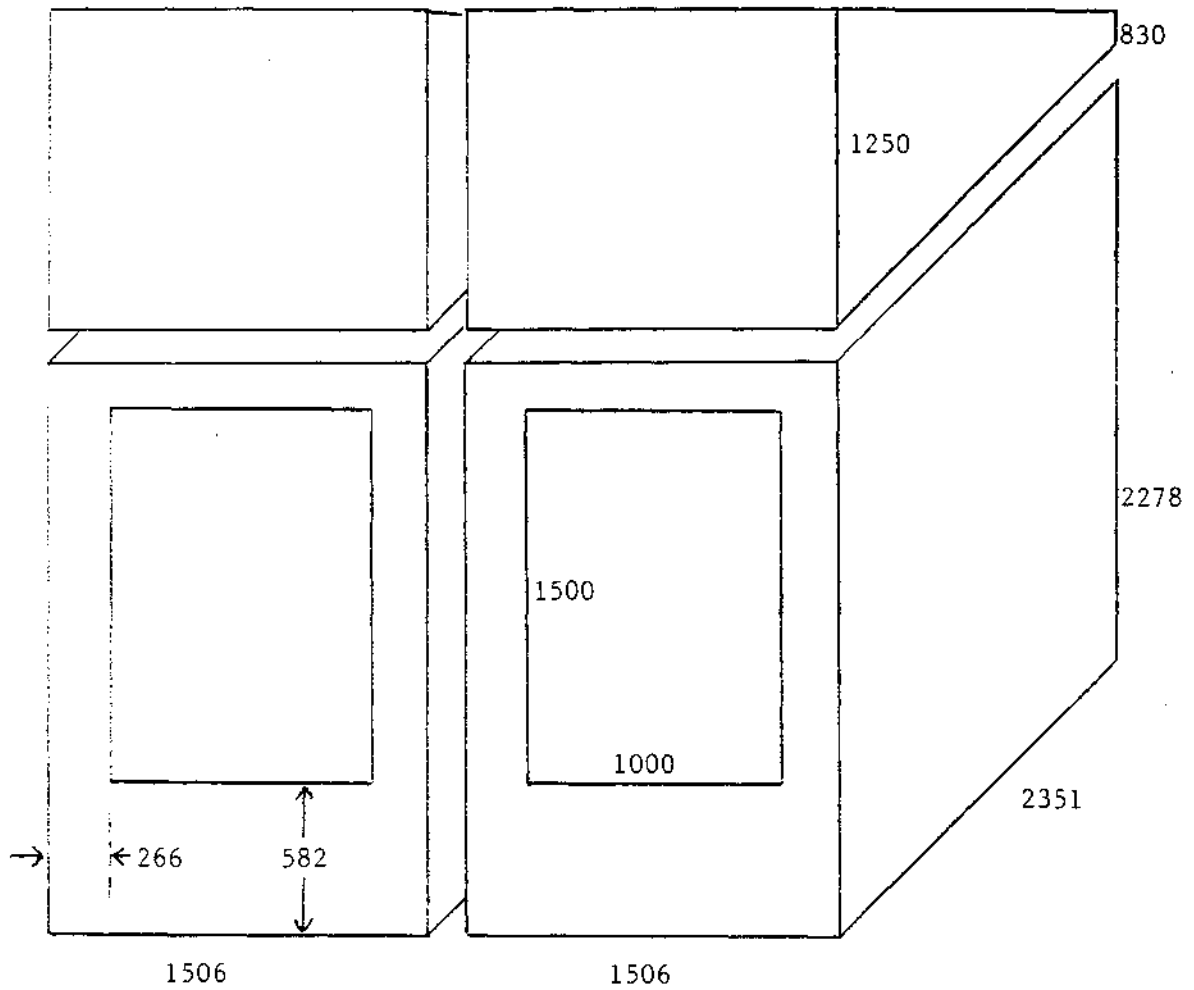


Figure 4.1: Test building internal geometry
(all dimensions mm)

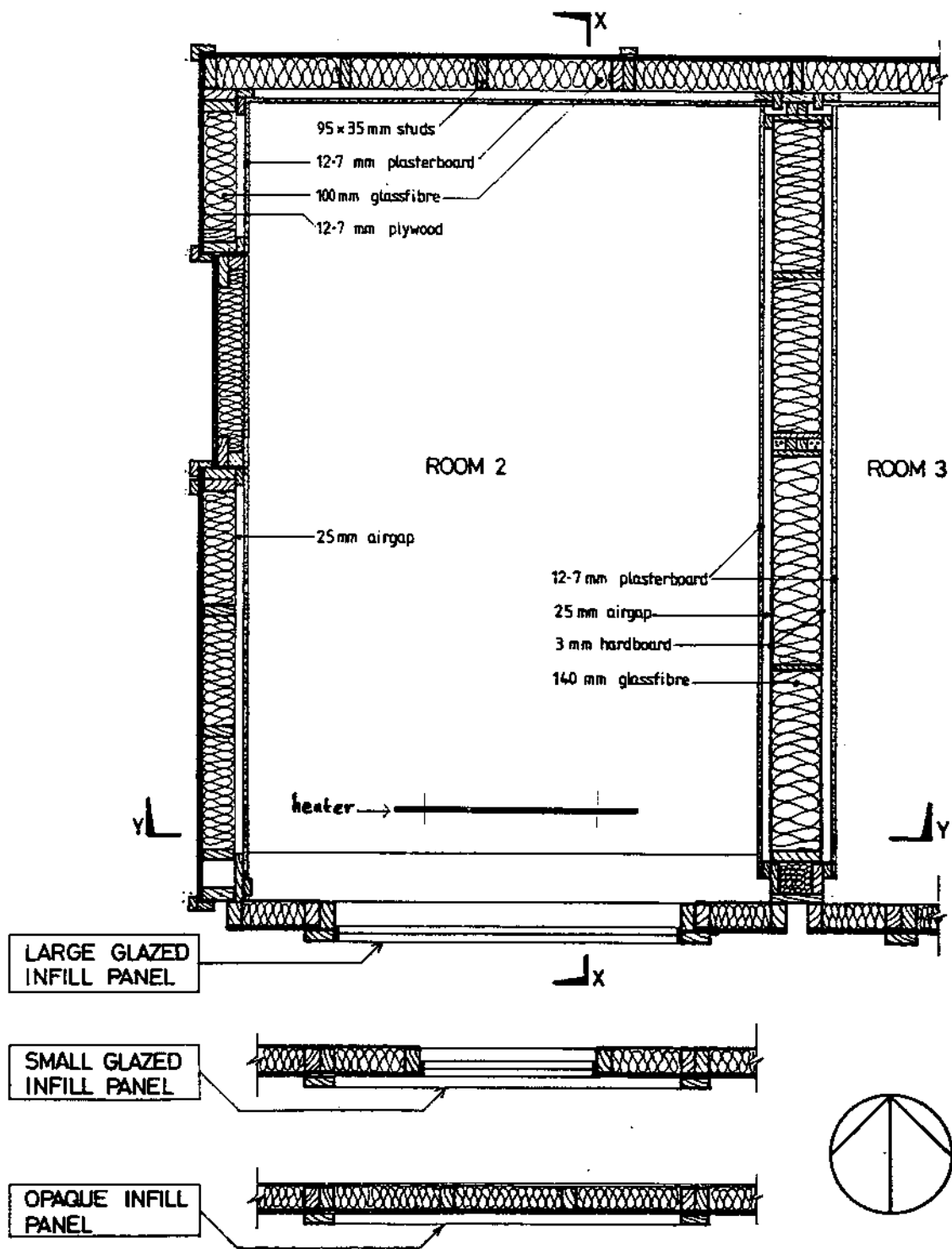


Figure 5.1: Plan view of test room showing construction

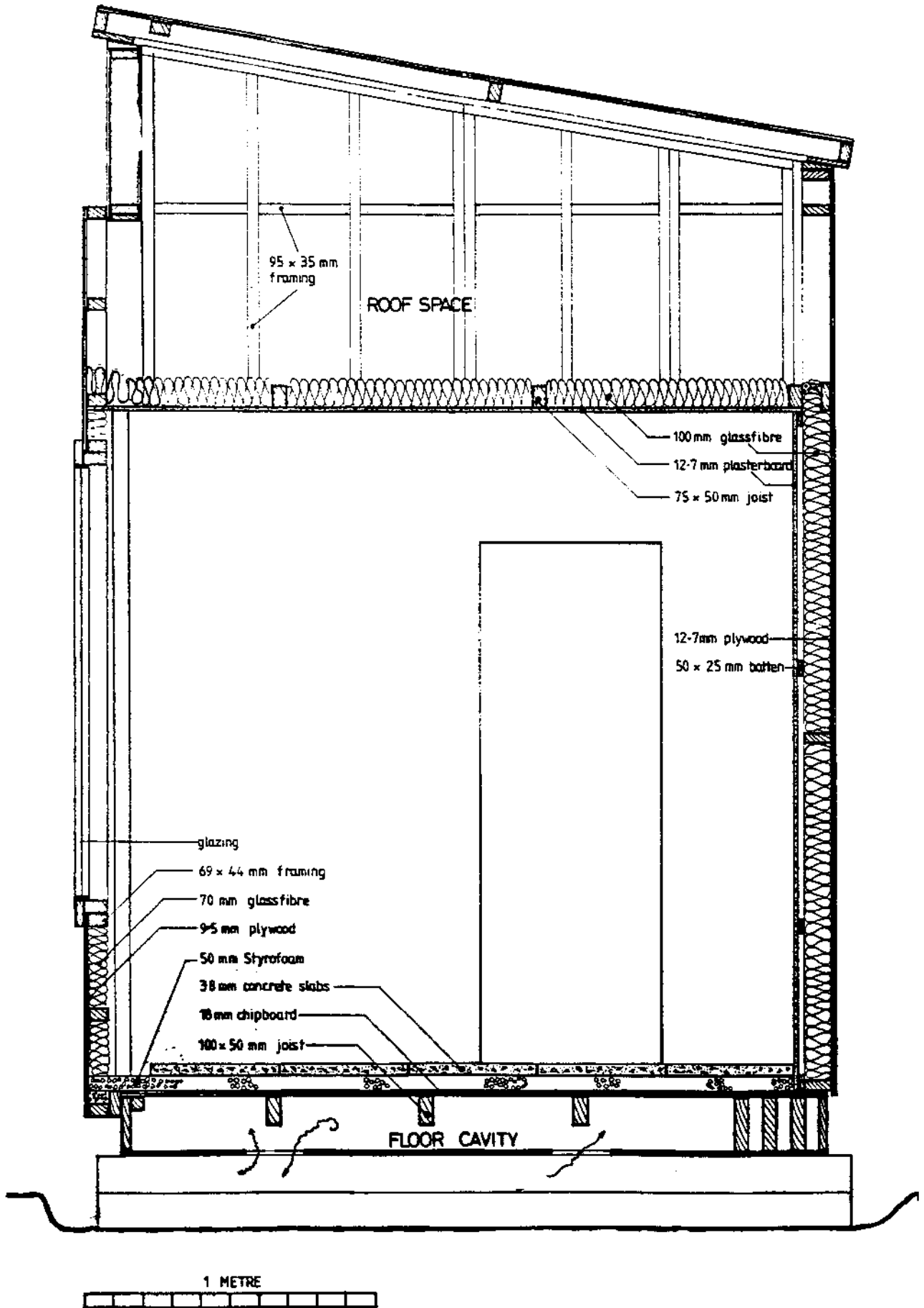


Figure 5.2: Section of test room on XX showing construction
(heater omitted)

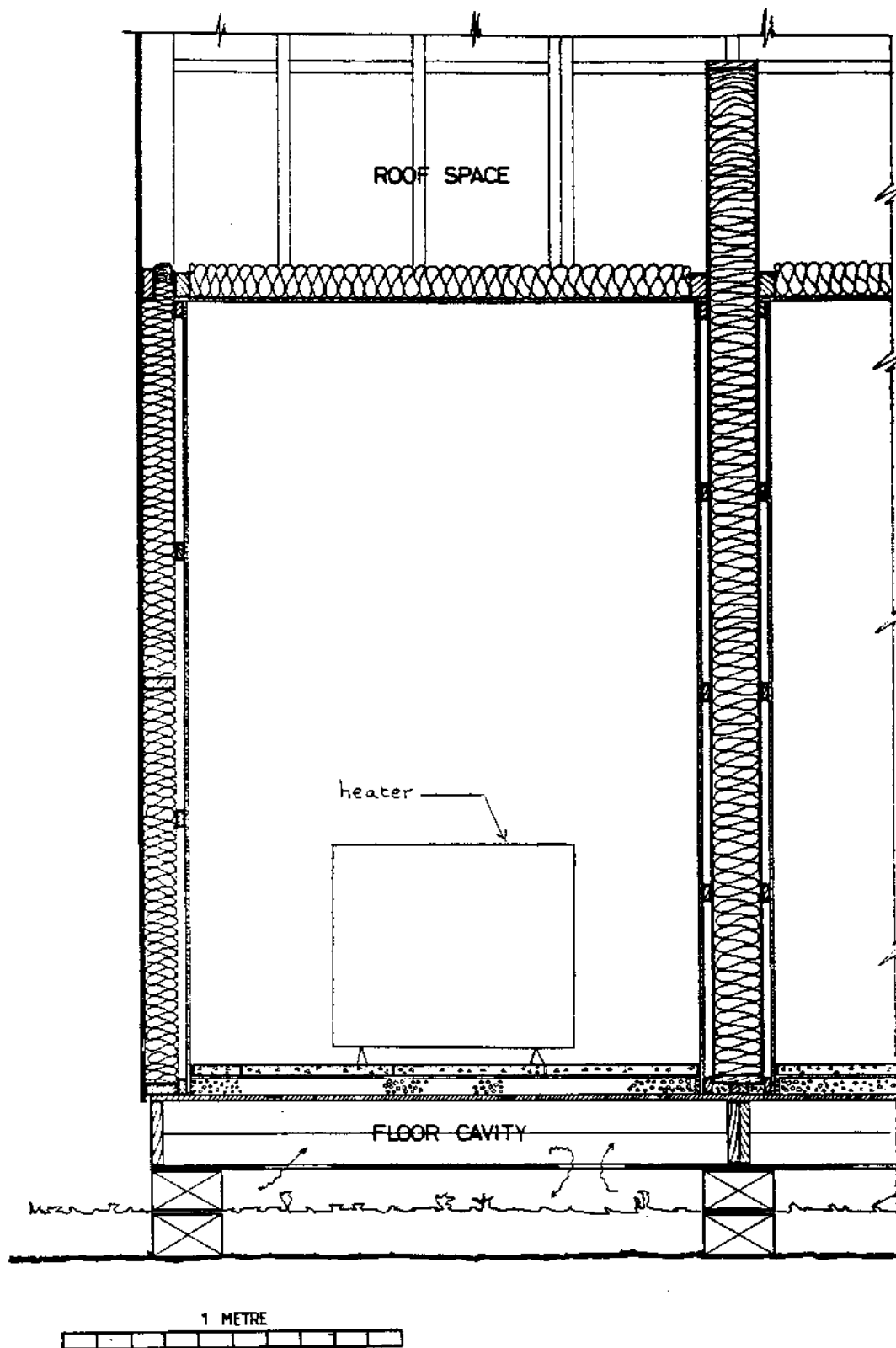


Figure 5.3: Section of test room on YY showing construction

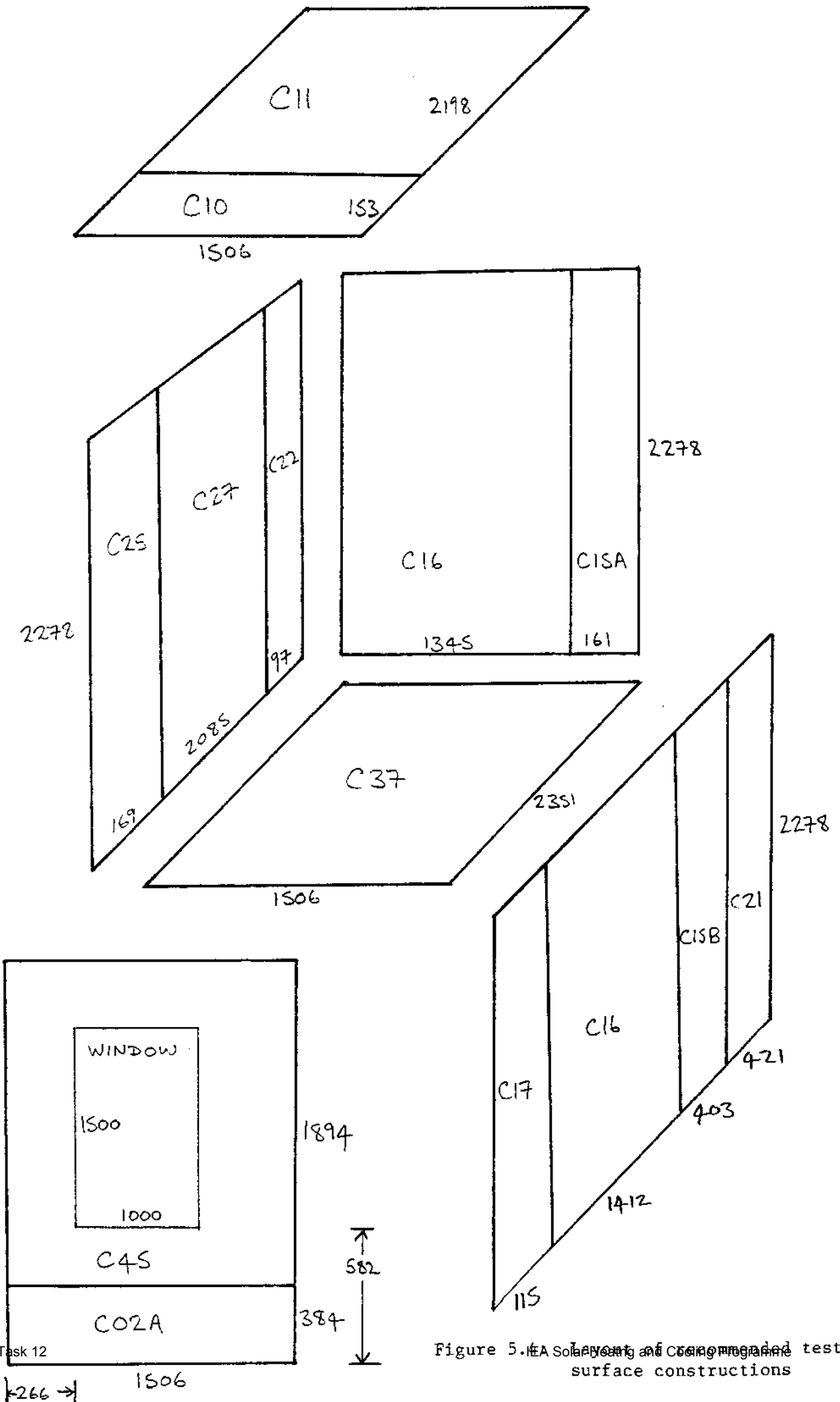


Figure 5. EA Solar Energy and Cooling program test room surface constructions

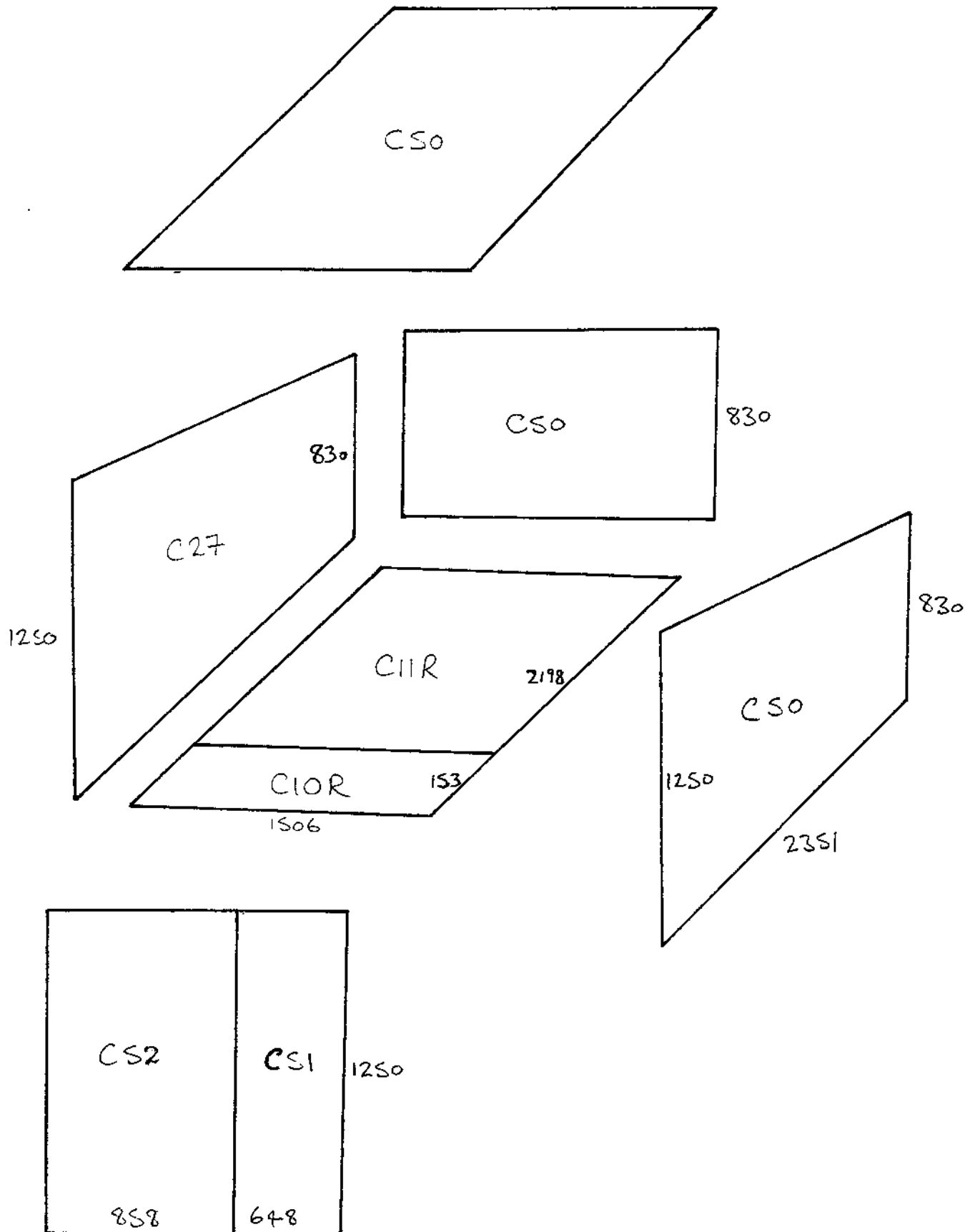


Figure 5.5: Layout of recommended roofspace surface constructions

recommended to represent rooms 1, 3 and 5, and Figure 5.5 shows the layout of surfaces in each roofspace. The room constructions include elements which have had their properties modified to take account of the three dimensional heat flow effects which occur in the corners of the rooms, denoted by the symbol [A]. The way in which these modifications were derived is described in full in Appendix 1 to this Site Handbook. (No attempt has been made to account for two or three-dimensional heat flows near joists and wood frames in the outer of each surface. However it is thought that this uncertainty is covered by the large allowance for edge effects (see section 8)).

5.1 Test room construction details

Table 5.1 summarises the finish of each surface in terms of solar absorptivity and longwave emissivity. These values have been estimated from tabulated data, except for the internal solar reflectances which were measured in the laboratory [1]. The table also acts as an index to Tables 5.2 to 5.9 which give the construction and thermal properties of each of the room surfaces.

Surface	Area m ²	Internal finish		External finish		Construction table
		Solar absorptivity	Emissivity	Solar absorptivity	Emissivity	
Floor	3.541	0.50	0.9	0 [†]	0.9	5.2
North wall	3.431	0.16 ^[1]	0.9	0.16	0.9	5.3
East wall	5.356	0.16 ^[1]	0.9	0.16	0.9	5.4
South wall	3.431	0.16 ^[1]	0.9	0.16	0.9	5.5, 5.8, 5.9
West wall	5.356	0.16 ^[1]	0.9	See main text		5.6
Ceiling	3.541	0.16 ^[1]	0.9	0.4	0.9	5.7

[†]Although the solar absorptivity of the exterior floor surface is 0.5, this should be modelled as 0. This is to avoid any ground reflected solar radiation impinging on the underside of the floor, which faces a dark cavity, during the simulation

Table 5.1: Test room surface finishes

Tables 5.2 to 5.7 contain details of the surface constructions which are common to all the test rooms. In all the construction tables the layers making up each construction are listed starting outside the zone and working inwards. Wherever possible, material properties supplied by the material manufacturers have been quoted [2]. Where such data could not be obtained standard sources have been used [1,3], and the source is referenced in each table.

Code	Area m ²	Material	Conductivity W/mK	Density kg/m ³	Specific heat J/kgK	Thickness m
C37	3.541	Chipboard	0.140	720	1300 ^[3]	0.018
		Styrofoam	0.027	34	1404	0.050
		Concrete	1.280	2000	920	0.038

Table 5.2: Test room Floor construction

Code	Area m ²	Material	Conductivity W/mK	Density kg/m ³	Specific heat J/kgK	Thickness m	
C15A	0.367	Plywood	0.181	576	1210 ^[3]	0.013	
		WoodA ^[A]	0.629	610	1380	0.095	
		Airgap					0.025
		Plasterboard	0.150	860	1090 ^[3]	0.013	
C16	3.064	Plywood	0.181	576	1210 ^[3]	0.013	
		Rockwool	0.043	12	840 ^[3]	0.100	
		Airgap					0.020
		Plasterboard	0.150	860	1090 ^[3]	0.013	

Table 5.3: Test room North wall construction

Code	Area m ²	Material	Conductivity W/mK	Density kg/m ³	Specific heat J/kgK	Thickness m	
C15B	0.918	Plywood	0.181	576	1210 ^[3]	0.013	
		WoodB ^[A]	0.253	610	1380	0.095	
		Airgap					0.025
		Plasterboard	0.150	860	1090 ^[3]	0.013	
C16	3.217	Plywood	0.181	576	1210 ^[3]	0.013	
		Rockwool	0.043	12	840 ^[3]	0.100	
		Airgap					0.020
		Plasterboard	0.150	860	1090 ^[3]	0.013	
C17	0.262	Plywood	0.181	576	1210 ^[3]	0.013	
		Airgap					0.095
		Wood	0.125	610	1380 ^[3]	0.025	
		Plasterboard	0.150	860	1090 ^[3]	0.013	
C21	0.959	Plywood	0.181	576	1210 ^[3]	0.013	
		Rockwool	0.043	12	840 ^[3]	0.076	
		Plasterboard	0.150	860	1090 ^[3]	0.013	

Table 5.4: Test room East wall construction

Code	Area m ²	Material	Conductivity W/mK	Density kg/m ³	Specific heat J/kgK	Thickness m
C02A	0.578	WoodC ^(A)	0.205	610	1380	0.110
C45	1.352 [†]	Plywood	0.181	576	1210 ^[2]	0.010
		Rockwool	0.043	12	840 ^[3]	0.070

[†]All cases except Room 5 during the heated period (0.75m² double glazing), where the area of C45 is 2.102m².

Table 5.5: Test room South wall construction

The west wall of each room is the party wall with the adjacent test room. As described previously experiments are normally configured in such a way that the conditions in adjacent rooms are similar. Taken together with the fact that the party wall is highly insulated the overall heat flow through the wall can reasonably be assumed to zero. It is therefore possible to model the performance of a single test room, without needing to know the conditions in the adjacent room. Models which do not use a full geometric representation of a building may allow the user simply to omit the party wall. However, this will introduce significant errors because the thermal mass of the wall will be omitted from the room. The preferred approach is to model one half of the wall section, and to set the heat flow behind that construction to zero. Some models allow the user to define such adiabatic surfaces directly, but if this facility is not available the same effect can be achieved by placing a highly insulating layer behind the construction. In the table below this layer is denoted R-999. Some models may allow such resistances to be entered directly, if not a fictitious material with a high resistance may have to be defined.

Code	Area m ²	Material	Conductivity W/mK	Density kg/m ³	Specific heat J/kgK	Thickness m
C22	0.221	R-999				
		Foam	0.027	34	1404	0.045
		Wood	0.125	610	1380 ^[3]	0.053
		Plasterboard	0.150	860	1090 ^[3]	0.013
C25	0.385	R-999				
		Wood	0.125	610	1380 ^[3]	0.073
		Airgap				0.025
		Plasterboard	0.150	860	1090 ^[3]	0.013
C27	4.750	R-999				
		Rockwool	0.043	12	840 ^[3]	0.073
		Airgap				0.025
		Plasterboard	0.150	860	1090 ^[3]	0.013

Table 5.6: Test room West wall construction

Code	Area m ²	Material	Conductivity W/mK	Density kg/m ³	Specific heat J/kgK	Thickness m
C10	0.230	Wood	0.125	610	1380 ^[3]	0.075
		Plasterboard	0.150	860	1090 ^[3]	0.013
C11	3.310	Rockwool	0.043	12	840 ^[3]	0.100
		Plasterboard	0.150	860	1090 ^[3]	0.013

Table 5.7: Test room Ceiling construction

Table 5.7 completes the description of the construction common to all the test rooms. Table 5.8 describes the construction of the south facing window panel installed in each of the three rooms.

Code	Area m ²	Material	Conductivity W/mK	Density kg/m ³	Specific heat J/kgK	Thickness m
Room 1: Double glazed						
DG	1.500	Glass	1.050 ^[4]	2500 ^[4]	750	0.004
		Airgap				0.006
		Glass	1.050 ^[4]	2500 ^[4]	750	0.004
Room 3: Opaque infil panel						
C45	1.335	Pty	0.181	576	1210 ^[3]	0.010
		Rockwool	0.043	12	840 ^[3]	0.070
C48	0.165	Plywood	0.181	576	1210 ^[3]	0.010
		Wood	0.125	610	1380 ^[3]	0.069
Room 5 - free-floating (May) period: Single glazed						
SG	1.500	Glass	1.050 ^[4]	2500 ^[4]	750	0.004
Room 5 - heated (October) period: Double glazed - as Room 1, but area = 0.75m ²						

Table 5.8: Test room alternative South facing glazing options

Table 5.9 gives the transmission properties of the glass used in the windows.

Refractive index	1.526
Extinction coefficient (/mm)	0.030
Thickness (mm)	4.00

Table 5.9: Transmission properties of glass

5.2 Roofspace construction details

Table 5.10 gives the details of the surfaces which make up the test room roofspace, and again acts as an index to Tables 5.11 to 5.16 which describe the constructions of those surfaces.

Surface	Area m ²	Internal finish		External finish		Construction table
		Solar absorptivity	Emissivity	Solar absorptivity	Emissivity	
Floor	3.541	0.40	0.9	0.16	0.9	5.11
North wall	1.250	0.40	0.9	0.16	0.9	5.12
East wall	2.445	0.40	0.9	0.16	0.9	5.13
South wall	1.883	0.40	0.9	0.16	0.9	5.14
West wall	2.445	0.40	0.9	See main text		5.15
Ceiling	3.596	0.40	0.9	0.90	0.9	5.16

Table 5.10: Roofspace surface finishes

Code	Area m ²	Material	Conductivity W/mK	Density kg/m ³	Specific heat J/kgK	Thickness m
C10R	0.230	Plasterboard	0.150	860	1090 ^[3]	0.013
		Wood	0.125	610	1380 ^[3]	0.075
C11R	3.310	Plasterboard	0.150	860	1090 ^[3]	0.013
		Rockwool	0.043	12	840 ^[3]	0.100

Table 5.11: Roofspace Floor construction

The constructions given in Table 5.11 are, of course, simply those of Table 5.7 in reverse order. Some models may require that these reversed constructions are explicitly defined, others may not. Take care not to replicate the construction inadvertently!

Code	Area m ²	Material	Conductivity W/mK	Density kg/m ³	Specific heat J/kgK	Thickness m
C50	1.250	Plywood	0.181	576	1210 ^[3]	0.013

Table 5.12: Roofspace North wall construction

Code	Area m ²	Material	Conductivity W/mK	Density kg/m ³	Specific heat J/kgK	Thickness m
C50	2.445	Plywood	0.181	576	1210 ^[3]	0.013

Table 5.13: Roofspace East wall construction

Code	Area m ²	Material	Conductivity W/mK	Density kg/m ³	Specific heat J/kgK	Thickness m
C52	1.073	Plywood	0.181	576	1210 ^[3]	0.010
C51	0.810	Plyonstud	0.125	610	1380 ^[3]	0.088

Table 5.14: Roofspace South wall construction

Table 5.15 contains details of the partition separating the two halves of the roofspace above the test rooms. Once again the notation R-999 has been used to denote a layer of very high thermal resistance.

Code	Area m ²	Material	Conductivity W/mK	Density kg/m ³	Specific heat J/kgK	Thickness m
C27	2.445	R-999				
		Rockwool	0.043	12	840 ^[3]	0.073
		Airgap				0.025
		Plasterboard	0.150	860	1090 ^[3]	0.013

Table 5.15: Roofspace West wall construction

Code	Area m ²	Material	Conductivity W/mK	Density kg/m ³	Specific heat J/kgK	Thickness m
C53	3.596	Roofing Felt	0.190	960	837	0.002
		Plywood	0.181	576	1210 ^[3]	0.013

Table 5.16: Roof construction

5.3 Distribution of solar radiation within the test rooms

The distribution on the various surfaces within the test rooms of the solar radiation entering the test rooms with windows should be modelled as accurately as possible. However, some simulation models, for example SERIRES, require this information as input. Considerable work has been carried out in the test rooms to determine these distributions, and a simple algorithm, DIST12, has been produced to allow them to be predicted [5]. Appendix 2 gives the predicted distributions from DIST12 for the glazed rooms in the configurations employed here. These are for guidance only.

5.4 Infiltration

The test rooms were designed to be very tightly sealed, in order to eliminate potentially uncertain air infiltration. The measures used to achieve this are detailed in part 3 of the Validation Package, the Quality Assurance report. When an experiment requires it, ventilation air can be drawn into the rooms at a carefully metered, constant, rate. This facility was not used for any of the datasets described in this document. The air change rate within all the test rooms should thus be assumed to be zero.

The roofspaces are ventilated by gaps in the building eaves on the north and south faces. An air change rate of 1 ac/h may be assumed for each roofspace.

5.5 Heat source characteristics

The test rooms are each heated by an oil-filled electric panel radiator. The average maximum power output of these radiators is 680 W, with deviations of approximately ± 20 W from this figure for individual units. The heat transfer characteristics of the radiators have been calculated using standard empirical results for the convective and radiative heat transfer from a vertical heated plate. It was concluded that the heat output from the radiator was 60% radiant and 40% convective. The resulting predictions of surface temperature for a given total heat output have been compared with the measured temperature of the radiator and found to be in good agreement, lending some credibility to the calculation [6].

The dynamics of the heat source were identified in a short experiment in which the heater was switched pseudo-randomly at five minute intervals for a period of ten days. Cross correlation techniques were then used to extract the dynamic response of the heater in terms of its impulse and step responses. It was concluded that the dynamics of the heater could be well represented by a first order system with a time constant of 22 minutes [6].

Table 5.17 summarises the above results.

Heater type	Oil-filled electric panel radiator
Size	0.68 m (l) x 0.57 m (h) x 0.02 m (t)
Total surface area	0.810 m ²
Power output	680 W
Radiative/Convective split	60/40
Time constant	22 minutes

Table 5.17: Test room heater characteristics

The heater control units are industrial PID (Proportional + Integral + Derivative) units manufactured by Gulston, type 2070. The control parameters that we used were chosen after a simple system identification/controller tuning experiment. They are:

Proportional band	4.0°C
Integral time	99 minutes 59 seconds
Derivative time	15 minutes

Thermal simulation programs usually assume that the air within a zone is well mixed. This may not always be the case and may influence the interpretation of the results.

6 DATA ACQUISITION SYSTEM

Data is collected on the test site by a centralised data acquisition system. The system is built around an IBM-AT Personal Computer equipped with a 40 Mbyte hard disk.

The data acquisition computer is interfaced to a digital voltmeter and multi-channel multiplexer via a high speed RS232 link. The digital voltmeter records voltages from solarimeters and temperature sensors, and also periodically checks its own calibration by measuring the output of a voltage reference source.

The data acquisition computer is also interfaced to 16 pulse counting units, which allow the outputs of the test room electricity and ventilation air meters to be recorded.

Finally, the data acquisition system also controls the operation of the test room heating and ventilating systems. The heat source in each room is controlled by a commercial Proportional + Integral + Derivative control system which is switched by the data acquisition system. The control parameters used in these units have been optimised for the test rooms to obtain a high standard of temperature control (typically to within $\pm 0.2^{\circ}\text{C}$) in the *face* of large disturbances such as incoming solar radiation. Control can be based on the air temperature at the centre of the test room, on black globe temperature, or on any mix of the two.

The data acquisition system is operated by software developed over a period of some years by EMC. The software allows:

- sampling from sensors at different rates, depending on the time constant of the sensor, calibration functions can be applied immediately to convert the output of sensors into engineering units, the control of heating and ventilation systems using either deterministic heater schedules or pseudo-random heater operating sequences,
- real-time graphical displays of all measured quantities and their history, allowing rapid checks to be made on the function of all sensors and systems, and
- the transfer of data from the machine whilst data acquisition is underway, either via a network connection to another PC or direct to floppy disk for archiving.

The entire data acquisition and control system is powered by an uninterruptible power supply which serves to clean the incoming mains supply and also gives approximately 15 minutes operation in the event of a power failure.

6.1 Timing of recorded data

The data supplied with this document is in the form of hourly average values. Each set of values is prefixed by a day number, calculated assuming that January 1st is day 1, and an hour number. The values are averages of measurements over the hour preceding the time given by the hour number. The first line in each file has hour number 1, and the data on that line thus relates to the period from midnight to 1:00 am on the first day of the experiment.

6.2 Sensor types, locations and accuracies

External air temperature is measured using an aspirated sensor, to ensure that the results are not influenced by solar radiation incident on the sensor. The same unit incorporates a wet bulb sensor which allows the relative humidity level to be derived.

Solar radiation is measured using Kipp and Zonen units as the principal sensors. However, secondary measurements are also made using Licor solid state devices, and these are used as a check that the Kipp and Zonen sensors are performing acceptably. One Kipp and Zonen and one Licor sensor are equipped with a shadow ring for the measurement of diffuse radiation. These are adjusted every three to four days, and all solarimeters are cleaned at the same intervals.

Wind speed and direction are measured using a conventional three cup anemometer and wind vane. These units are mounted on a mast 10m above ground level. The outputs of the two sensors are measured every ten seconds, and the resulting wind velocity vector is resolved onto two of the four

surfaces of the test buildings. The total wind run into each of these four bins is totalled over the data recording period.

Inside the test rooms air temperatures are measured at three heights using solid state temperature sensors housed in radiation shields consisting of two concentric tubes coated with reflective Mylar. Black globe temperature is also measured in a matt black copper globe of diameter 150 mm. In the glazed test rooms a white polystyrene shield protects the globe sensor from direct solar radiation, and also serves to further shield the middle air temperature sensor. Surface temperatures are measured using the same semiconductor devices mounted in thin aluminium wells which are then bonded to the surface and painted to match. All surface sensors on a given surface are mounted on areas of the same construction type. Two sensors are mounted on the test room floor, ceiling and each side wall, and four on the back wall.

Electrical power input to each room is measured using a pulsed output electricity meter, situated in the room to eliminate errors due to voltage drops along the mains wiring to the rooms.

The Kipp and Zonen solarimeters are calibrated annually by the UK Meteorological Office. All temperature sensors are calibrated against an in-house Quartz reference thermometer which is in turn calibrated annually by the UK National Standards Organisation. The electrical power meters are calibrated using a dummy load and measurements of voltage and current from calibrated meters.

Table 6.1 gives the accuracies which can be expected from the sensors described.

Measured quantity	Sensor Manufacturer and type	Estimated accuracy
External air temp	Vector instruments H301/RS	$\pm 0.2^{\circ}\text{C}$
Wet bulb temp	Vector Instruments H301/RS	$\pm 0.2^{\circ}\text{C}$
Solar radiation	Kipp and Zonen CM5	$\pm 2\%$
Wind speed	Vector Instruments A100	$\pm 5\%$
Wind direction	Vector Instruments W200P	$\pm 5^{\circ}$
Internal air temp	Analog Devices AD590KH	$\pm 0.2^{\circ}\text{C}$
Internal globe temp	Analog Devices AD590KH	$\pm 0.2^{\circ}\text{C}$
Internal surface temp	Analog Devices AD590KF	$\pm 0.2^{\circ}\text{C}$
Electrical power consumption	Aron 60A Watt-Hour meter	$\pm 2\%$

Table 6.1: Sensor descriptions and accuracies

6.3 Data processing

All recorded data is first inspected graphically to check for outliers and sudden changes in values. The raw data is then processed to produce working data files of the type included with this document.

Solar radiation readings which are less than zero (due to longwave radiation from the Kipp and Zonen domes to the night sky) are set to zero. The outputs from the Kipp and Zonen solarimeters are then temperature compensated. Finally, a correction for the area of sky obscured by the two shadow bands is applied to the instruments measuring diffuse radiation. This correction varies with time of year. Finally, the readings of the Kipp and Zonen solarimeters are compared with those of the Licors as a final check.

Relative humidity is calculated from the wet and dry-bulb temperature readings using standard relations [3].

Wind speed is derived from the measured wind roses by adding their components together in quadrature and dividing by the number of seconds in the data interval. For applications which require it, 'average wind direction' is found using an algorithm which first identifies the bins with the greatest and second greatest wind runs. If these are in adjacent sectors the wind direction is found using the standard trigonometrical relation. If not the wind direction is assumed to be that corresponding to the bin containing the greatest run of wind.

Inside the test rooms the measured air temperatures are combined in a space weighted average to yield a test room bulk air temperature. At this stage any measures of stratification required can also be generated.

Finally, the measured surface temperatures are combined into an area weighted average for each surface.

7 DATA SETS

7.1 Data set periods

Meteorological data for two ten day periods are supplied in Part 4 of this document. The two experimental periods are uniquely identified by their volume numbers, 099 and 110. Table 7.1 gives the start and finish dates of each volume of data.

Volume number	Start		Finish	
	Date	Day number	Date	Day number
099	21st May 1990	141	30th May 1990	150
110	17th October 1987	290	26th October 1987	299

Table 7.1: Data set start and finish dates

7.2 Climate summaries for data sets

Figure 7.1 shows the external air temperature and relative humidity over data volume 099. Figures 7.2 and 7.3 show the measured solar radiation and wind parameters over the same period. Figures 7.4 to 7.6 show the corresponding quantities for data volume 110, with the exception of relative humidity, which was not measured as part of that experiment. Table 7.2 summarises the mean values of the measured climate parameters over the two periods.

Figure 7.1: V099: Air temperature and relative humidity

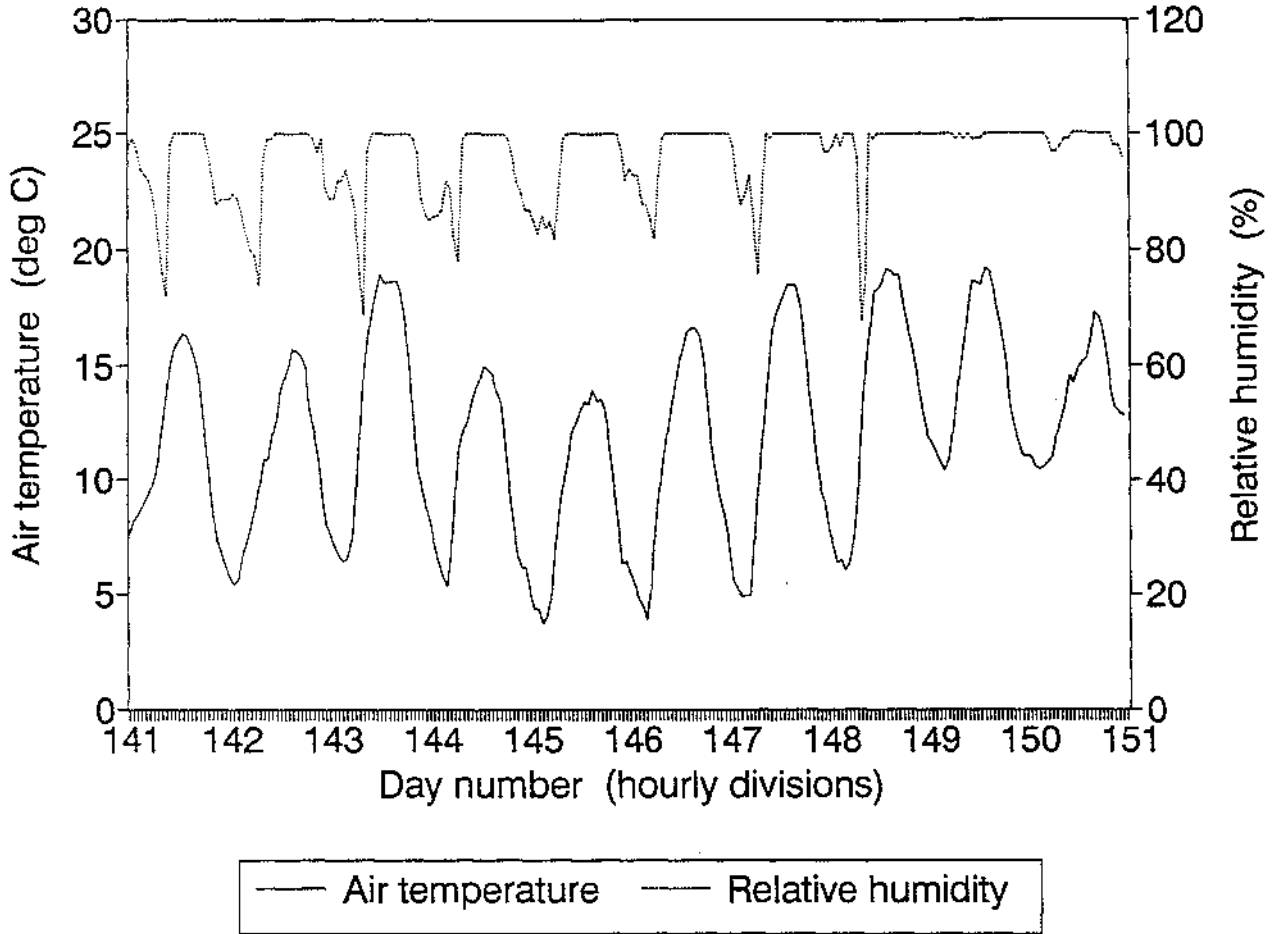


Figure 7.2: V099: Global and diffuse horizontal solar radiation

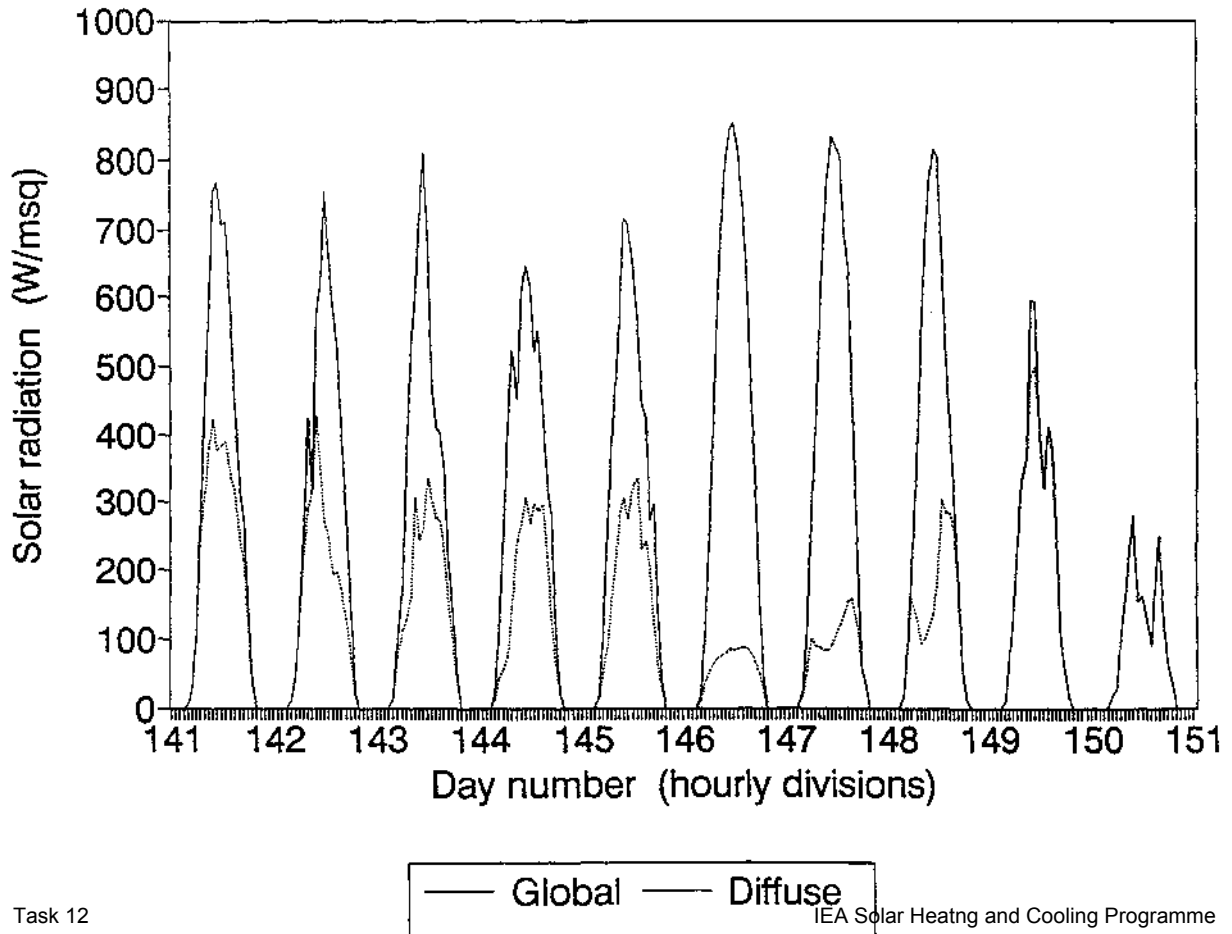


Figure 7.3: V099: Wind speed and direction

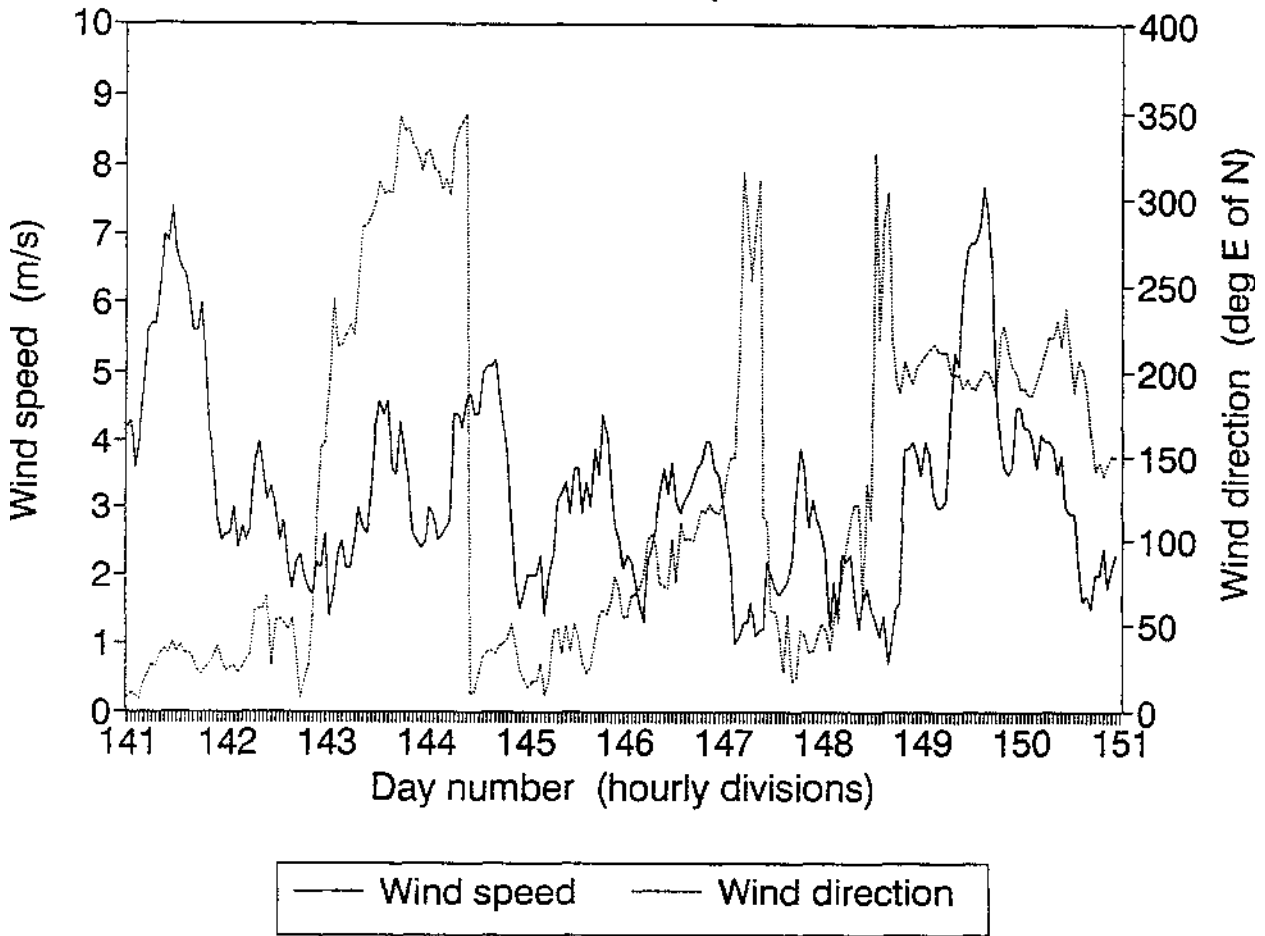


Figure 7.4: V110: Air temperature

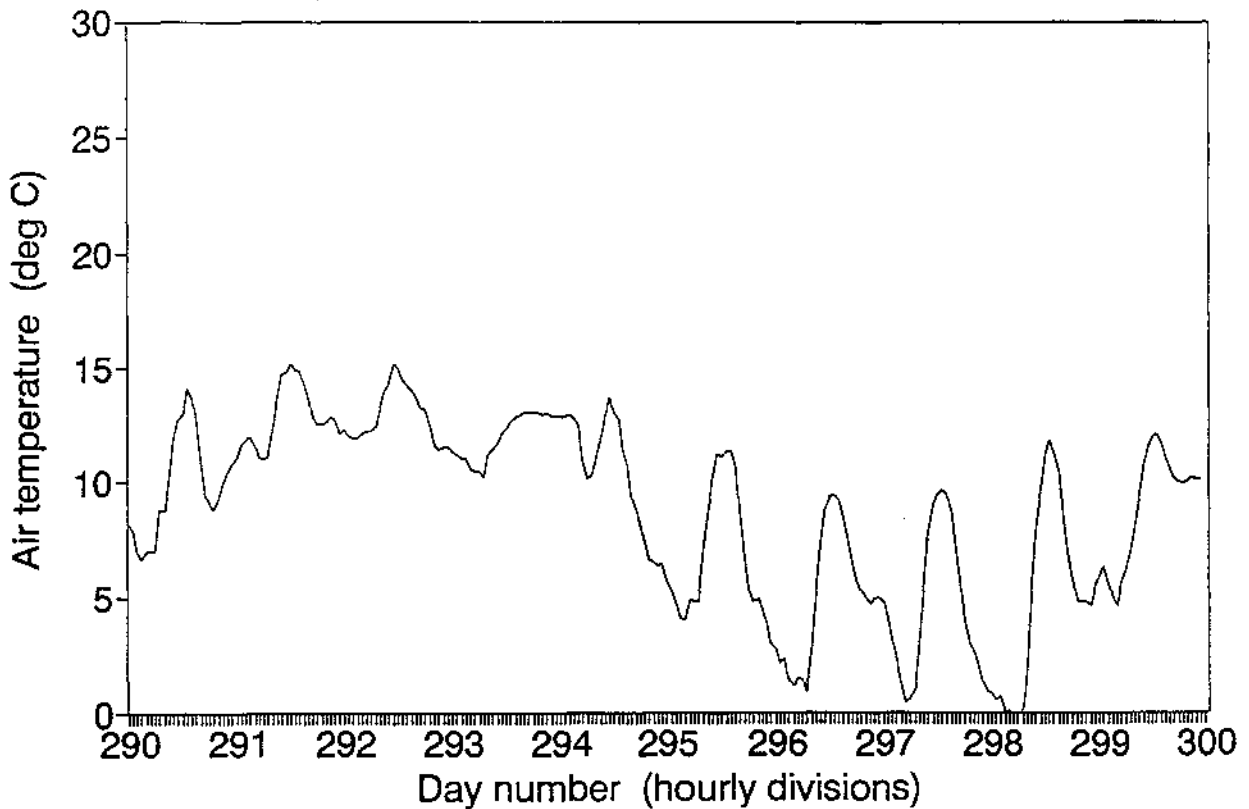


Figure 7.5: V110: Global and diffuse horizontal solar radiation

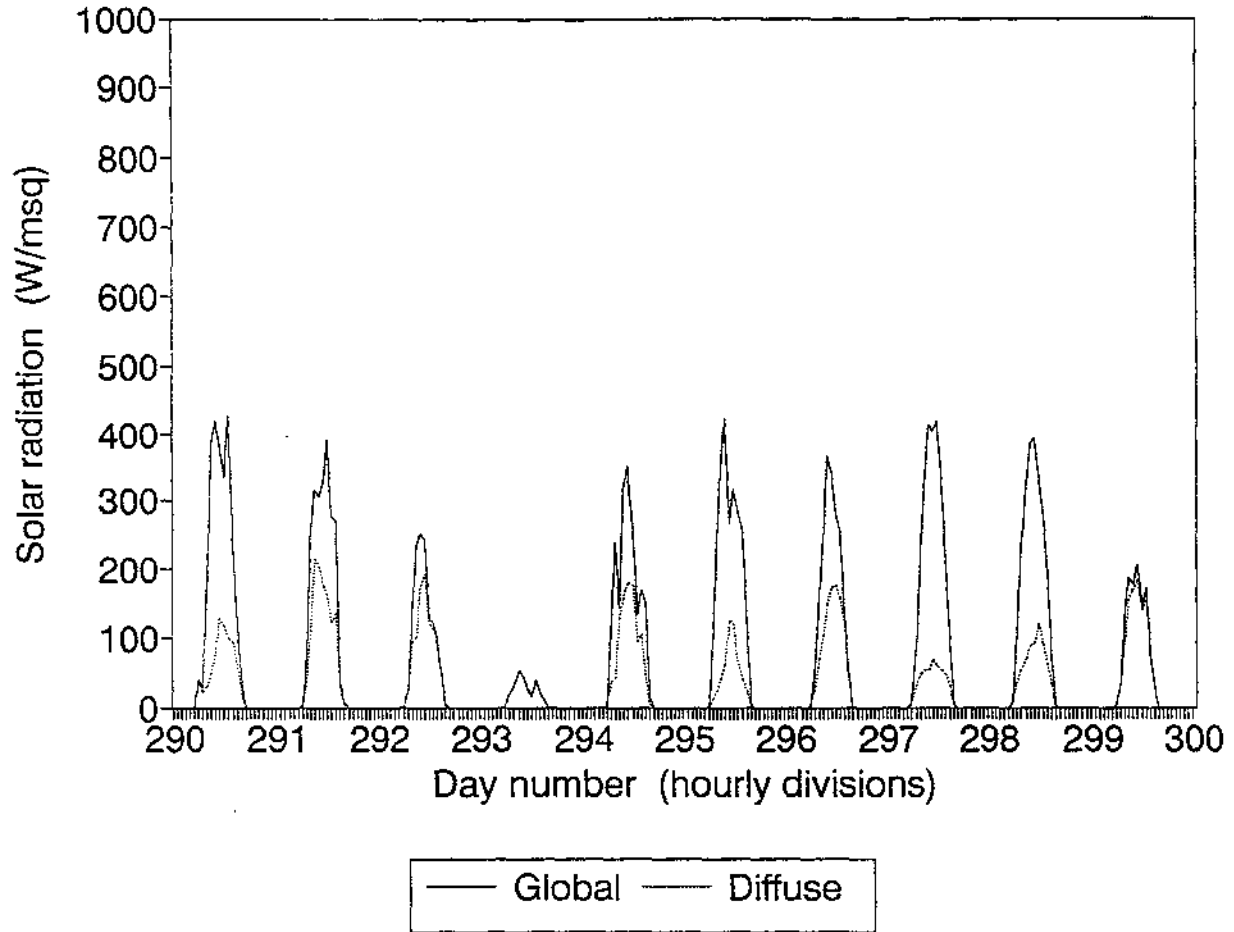
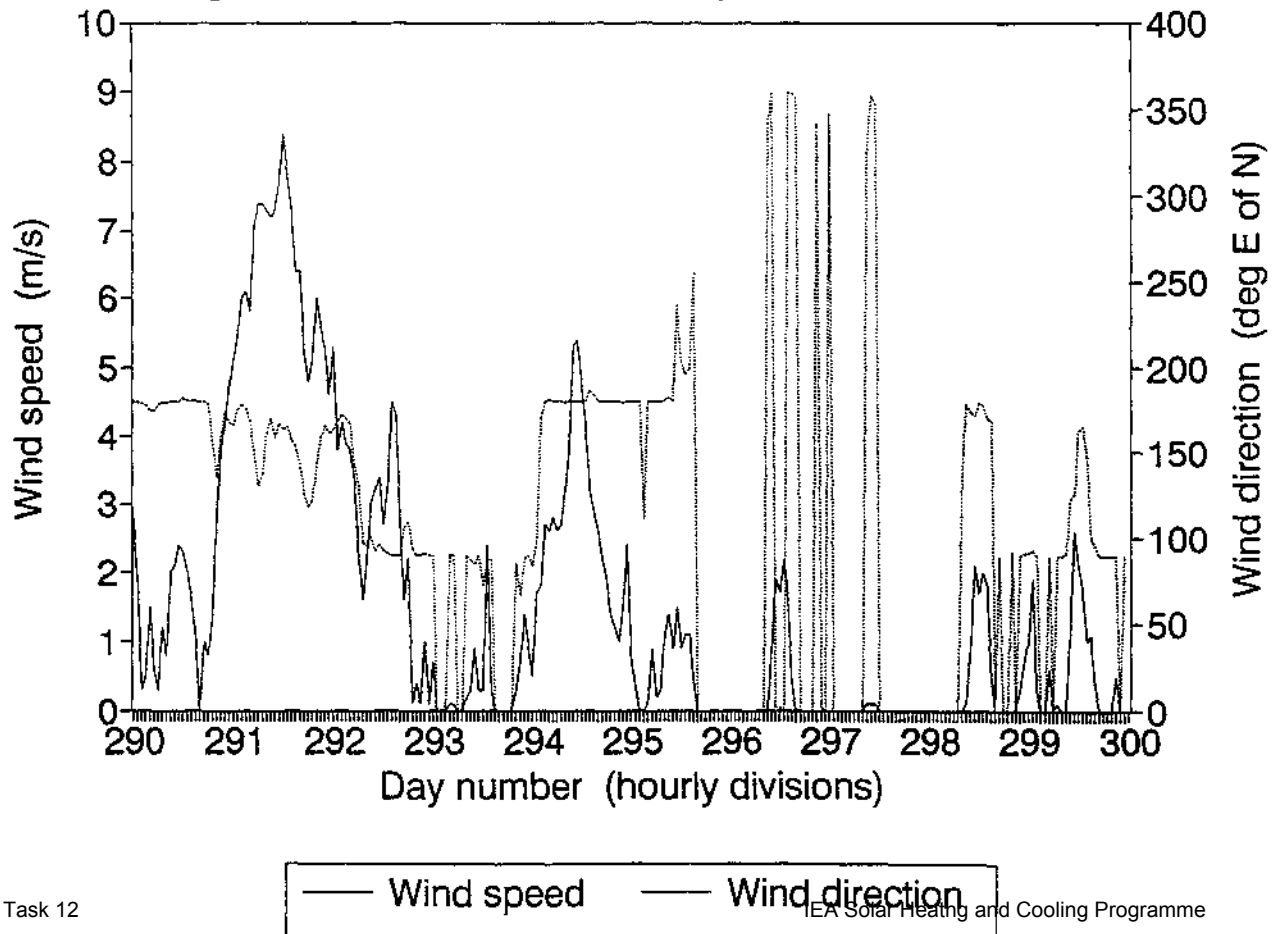


Figure 7.6: V110: Wind speed and direction



Volume number	External air temp °C	Relative humidity %	Global horizontal solar W/m ²	Diffuse horizontal solar W/m ²	Windspeed m/s
099	12.0	96	241	111	3.3
110	8.8	n/a	77	32	1.6

Table 7.2: Mean values of measured climate variables over experimental periods

7.3 Test room operation

Table 7.3 gives details of test room heater operation over the two experimental periods.

Volume number	Heater Schedule	Control temperature	Setpoint
099	Unheated		
110	6:00 - 18:00†	Shielded air temperature	30°C

†The heater is switched on at 6 o'clock in the morning and switched off at 6 o'clock in the evening. The heater is therefore in operation for 12 hours each day.

Table 7.3: Test room heater operation

7.4 Meteorological data file formats

Two meteorological data files were originally supplied with the Site Handbook. They each contain ten days meteorological data, for the periods defined in Section 7.1. The files are named V099.MET and V 110.MET and are in standard MS-DOS ASCII format. Each line contains data for one hour. The format of that data is detailed in Table 7.4. All times refer to GMT, no daylight saving hours were employed.

These files contain ½-hour-centred, hourly averaged, data constructed from 5-minute recordings. Because some programs require hour-centred weather data, additional files are provided on the Data Disk which is Part 4 of this document. These are described in Appendix 3.

Entry	Description	Units	Format
1	Day number		I5
2	Hour number		I5
3	Air temperature	°C	F5.1
4	Relative humidity	%	I5
5	Global horizontal solar radiation	W/m ²	I5
6	Diffuse horizontal solar radiation	W/m ²	I5
7	Wind speed	m/s	F5.1
8	Wind direction	°E of N	I5

Table 7.4: Meteorological data file formats

8 SENSITIVITY ANALYSIS

Modellers may wish to undertake sensitivity studies to account for the uncertainties in the experimental data. This will allow a more rigorous comparison between the predictions and measurements. To facilitate such studies, Table 8.1 lists the uncertainties in the parameters provided in the sections. Further explanations are given in Section 8.1. These values are to be used for sensitivity studies only, and not as replacements for the basic parameter values listed in the preceding sections.

Sensitivity analysis procedures are discussed in detail elsewhere. Such studies can be undertaken to investigate the sensitivity of a program to selected inputs, or to give the total uncertainty in one or more output parameters. It is important to note that, when the total uncertainty is obtained by adding the uncertainties due to the individual parameters (Differential Sensitivity Analysis), it must be calculated by adding the individual effects in QUADRATURE (and then taking the square root), i.e.

$$\Delta p_{tot} = \sqrt{\sum_{i=1}^I \Delta p_i^2}$$

where Δp is the difference between the prediction and the measurements, and I is the number of uncertain inputs.

When these data were used in the IEA Empirical Validation exercise, the alternative, and more rigorous, Monte Carlo Analysis Technique was used in conjunction with SERIRES to estimate the total uncertainty in the total heating energy (October Revised) and maximum and minimum temperatures (both periods). This work is more fully explained in Volume 1: Final Empirical Validation Report.

Table	Parameter	Nominal value	Uncertainty	Notes
Site Details				
3.1	Latitude	52.07°N	±0.05°	Note 1
3.1	Longitude	0.63°W	±0.05°	Note 1
3.1	Altitude	100 m	±5 m	Note 2
3.1	Ground reflectivity	0.20	±0.05	Note 3
3.1	Glazing orientation	9° W of S	±0.5°	Note 4
Test Room Surface Finishes				
5.1	External surface absorptivities	0.16	-0.06 +0.14	Note 5
5.1	Internal floor absorptivity	0.50	±0.10	Note 6
5.1	Internal other surface absorptivities	0.16	±0.02	Note 6
5.1	Internal and external emissivity	0.9	±0.05	estimate
Material Properties				
5.2	Styrofoam conductivity	0.027 W/mK	-0.002 +0.006 W/mK	Note 7
5.2	Concrete heat capacity	1840 kJ/K	±184 kJ/K	Note 8
5.3, 5.4, 5.5, 5.6, 5.7, 5.8	Rockwool conductivity	0.043 W/mK	±0.003 W/mK	Note 9
5.3, 5.4, 5.5, 5.6, 5.7, 5.8	Rockwool thickness	Various	±10 mm	Note 10
5.3, 5.4, 5.5, 5.6, 5.7, 5.8	Plasterboard heat capacity	937 kJ/K	±94 kJ/K	Note 11
5.4, 5.6, 5.7, 5.8	Wood conductivity	0.125 W/mK	±0.025 W/mK	Note 12
5.3, 5.4, 5.5	Edge effects-Wood A,B & C conductivity	Various	-0 +50%	Note 13
Glazing properties				
5.8	Glazed area	1.500 m ²	±0.02 m ²	Note 14
5.9	Glass extinction coefficient	0.030 mm ⁻¹	±0.005 mm ⁻¹	Note 13
n/a	Glazing cleanliness	1.00	-0.02 + 0.00	Note 14
Test Room Heater Characteristics				
5.17	Heater power	680 W	±40 W	Note 15
5.17	Heater R/C split	60/40	±10/10	Note 16
5.17	Heater time constant	22 minutes	±2 minutes	Note 16
n/a	Test room ventilation rate	0.00 ac/h	-0.00 + 0.05 ac/h	Note 17
n/a	Stratification of air	Variable	max. ±1.2°C	Note 18
7.3	Setpoint	30°C	±0.2°C	Note 19

Table 8.1: Uncertainty in the parameters supplied in this Site Handbook

8.1 Notes about Parameter Uncertainties

1. The location of the site was originally derived from the local Ordnance Survey sheet¹. It has subsequently been measured using the satellite Global Positioning System¹ and this measurement was found to agree with the figures derived from the map to within 0.002°. The figure given in the table thus represents a very pessimistic estimate of the uncertainty in the location of the test rooms.
2. The site is located in relatively flat countryside. A 100 m contour passes within approximately 200 m of the test buildings. In addition to this, the height of the centre of the main runway of the adjacent airfield (which is 1700 m the other side of the test buildings) is known to be 111 m. Taken together, these pieces of information allow us to estimate the uncertainty in the site altitude as ± 5 m.
3. The uncertainty assumed is in line with that chosen in previous studies^{1, 0}
4. The orientation of the test rooms has now been measured using several different techniques, and the figure given in the table again represents an extremely pessimistic estimate of the uncertainty in this figure.
5. The error band given is intended to account for the possibility of dirt on the external surfaces of the test rooms. In fact the surfaces were clean at the time these datasets were collected, and this therefore represents a very pessimistic estimate of the uncertainty in this parameter.
6. The solar reflectance of the white paint used on the test room walls and ceiling was measured by spectrophotometry, after conditioning the samples inside the test rooms^{1, 11}. The absorptivity of the test room floor was not measured directly, but the paint manufacturer's tabulated figure for the reflectance was 0.494¹. ~~lists the~~ reflectance of this shade as 0.42. Subsequent comparison with other manufacturer's data for paints of ostensibly the same shade also produced a value of 0.42¹, although this may, of course, have been taken directly from the Standard. For these reasons the relatively large uncertainty shown in the table has been assumed.
7. The conductivity of Styrofoam was supplied by the material manufacturer^[15], who will have measured it to an accuracy of $\pm 3\%$. However, there is known to be some variation between batches of this material, and after further discussion with the manufacturer this was assumed to add a further -5% +20% to the uncertainty in the properties of the material actually installed.
8. The density of the concrete slabs used in the test rooms was measured on site by weighing a number of slabs. The density was then calculated assuming nominal dimensions, removing this source of uncertainty from the simulation process. The remaining uncertainty comes from the use of the manufacturer's figure for the material specific heat capacity.
9. The approach taken to assess the conductivity of the Rockwool installed in the rooms follows that for Styrofoam (Note 5). The manufacturer's quoted value is again assumed to have been measured to an accuracy of $\pm 3\%$ ^[16]. Variations between batches of the material are assumed to add a further $\pm 4\%$ to this figure.
10. This value was determined by measurement. That measurement has subsequently been repeated (see Validation Package, Part 3: Quality Assurance Report) and the value originally obtained determined to be adequate.

11. The rationale behind the uncertainty assumed here follows that for the capacity of the concrete floorslabs (see Note 8).
12. Estimate of softwood conductivity uncertainty is hard to derive. The value quoted (0.125) is the CIBSE A3^[5] value for Deal. CIBSE gives 0.13 for generic 'Softwood' and 0.105 for Spruce. ASHRAE^[4,p] gives values for Spruce-Pine-Firs from 0.107 to 0.130. On seeing the large variation in quoted values a rather large uncertainty range was chosen.
13. The treatment of the test room edge effects is acknowledged to be approximate in Appendix 1. Not all edges are treated, and those which are have been assumed to be of only two types. The resulting uncertainty was originally estimated in the IEA exercise as $\pm 30\%$. Subsequent discussions with Martin Gough, of EDSL Ltd, have identified a number of reasons why this may not be sufficient. In particular, the front edge of the room adjacent to the party wall is likely to have a much higher loss than that assumed. Together with the fact that not all edges were treated this suggests that the published edge effects are very unlikely to be overestimates, and the uncertainty estimate has been modified to $-0/+50\%$.
14. The area of the test room glazing is in some cases slightly reduced by the intrusion of the double glazing spacer unit into the window aperture (see Part 3: Quality Assurance Report), and this effect has been accounted for by assuming a small uncertainty in the size of that aperture. The glazing was cleaned every few days during data collection. However, a small allowance has been made for the fact that some dirt may have accumulated. This has been simulated by incorporating an additional uncertainty in the transmission, of between 100% (implying clean glass) and 98% (implying a small amount of dirt). The glazing extinction coefficient was deduced from the manufacturer's figure for the normal transmission of a single pane of the glass, and the assumed uncertainty reflects the uncertainty in the measured transmission. The thickness of the glass has been measured to a high degree of accuracy, and the small uncertainty which remains is effectively absorbed into the uncertainty assumed for the extinction coefficient.
15. The uncertainty in the measurement of the delivered heater power is small, at $\pm 2\%$ (see Table 6.13). However, there are significant production tolerances in the power outputs of the heaters in different rooms, and there are variations in power output with the surrounding environment. The figure shown has been derived by examining the peak power consumption of each room over the course of many days.
16. The heater R/C split and time constant were derived from a combination of calculation and measurement. The radiative and convective outputs of the panel were calculated, and used to derive the R/C split. The total power output at a given temperature was then compared with the result of this calculation and found to be within 2%, lending some credibility to the calculation. On the basis of this result the uncertainty in the proportion of the heat output which is, say, radiant, is believed to be less than $\pm 10\%$. The heater time constant was derived by operating the heater pseudo-randomly and deriving the step response of the surface temperature to power input. The step response was found to be well represented by a first order system with a time constant of 22 minutes. The uncertainty in determining this time constant was ± 2 minutes.
17. The measures taken to ensure the airtightness of the rooms are described in detail in Part 3: Quality Assurance Report.
18. In order to assess the vertical stratification of the room air, the differences between the three air temperature readings were investigated. The maximum difference was found to be 2.4°C during a short period in the double glazed heated room. The differences were generally much smaller.

19. The uncertainty in the measurement of the control temperature, from which the setpoint is maintained, is the same as the uncertainty in the other temperature measurements, $\pm 0.2^\circ\text{C}$.

8.2 Further Comments on Parameter Uncertainty

The above table only contains uncertainties in fundamental physical properties. It was a policy of the IEA empirical validation exercise not to supply derived parameters which may be required by some programs, but to let the program users make their own decisions about appropriate values for such parameters. The same policy applied for the uncertainty in any derived parameters. Parameters falling into this category are, for example, window U-value and the air gap resistance.

This handbook lists numerous materials, with 4 parameters used to describe each one (conductivity, density, specific heat, thickness). Each of these parameters has some uncertainty associated with it. However, it would be a huge task to undertake a complete sensitivity analysis, taking due account of the possible links between parameters, e.g. the conductivity of mineral wool is related to its density etc.

Fortunately, a great deal of work was done in this area within an earlier UK study¹ Based on this work, and preliminary studies using SERI-RES², it is clear that only selected properties of certain materials were significant for these rooms. This is particularly so when the total sensitivity is approximated by adding individual effects in quadrature. This process suppresses very small individual sensitivities. Only the key parameters have therefore been listed in Table 8.1. Individual modellers may wish to confirm the truth of the foregoing statements by undertaking tests of their own using plausible material property uncertainties.

Uncertainties for some parameters are not listed at all:

- site exposure - because the input of this parameter is model specific;
- area of surfaces - because the sensitivity to any possible errors is very small;
- ceiling external absorptivity - because this is irrelevant since no solar radiation enters the roof space;
- glass refractive index - because the uncertainty is negligible; *and*
- roof air change rate - because the parameter was estimated. A range between 1 and 3 air changes per hour has been used previously (The roof space has only very small ventilation openings, so an infiltration rate higher than 3 is very unlikely). The impact of uncertainty in this parameter on the performance of the rooms below is also likely to be small because the ceilings of the rooms below are well insulated.

For the October measurement period, no information about external **relative humidity** was available. For programs which use this parameter, sensitivity studies could be undertaken, using values of 55% to 100%. This is an extreme range which is based on the weather data for October at Kew in London, UK. Values outside this range are very unlikely.

Concern had also been expressed in the past by some participants about the validity of the measured values for the May period. Again you may wish to include this period in your sensitivity analysis, using, as above, suggested values between 35 and 100%.

REFERENCES

- [1] Evaluation of the solar reflectance of four samples of painted cement. University College Cardiff. Department of Mechanical Engineering and Energy Studies. 1986.
- [2] Description of the EMC Test Room facility. 1987-88. EMC Report to ETSU. S1197-D. September 1988.
- [3] ASHRAE Handbook: 1989 Fundamentals, American Society of Heating and Refrigeration Engineers.
- [4] CIBSE Guide, Section A3 - Thermal Properties of Materials, Chartered Institute of Building Services Engineers, London, 1986,
- [5] TEST CELL STUDIES 1: Solar-distribution. A study of the way that incoming solar radiation is distributed between the elements of a room. EMC report to ETSU. S1162-P1.
- [6] Detailed Model Comparisons - A model validation exercise using SERI-RES. EMC Report to ETSU. ETSU S1197-P9. June 1991.
- [7] Sensitivity analysis techniques for building thermal simulation programs, K. Lomas and H. Eppel, Energy and Buildings, 19, (1992) pp.21-44
- [8] UK Ordnance Survey Sheet 153: Bedford and Huntingdon.
- [9] Sensitivity Analysis Techniques for Empirical Validation of Building Thermal Simulation Programs. K J Lomas and H Eppel. Presented at Workshop: Validation of Building Energy Models, Electricité de France, June 9& 10 1992.
- [10] An investigation into Analytical and Empirical Validation Techniques for Dynamic Thermal Models of Buildings Vol. 4. K J Lomas and N T Bowman. September 1987. UK Science and Engineering Council Report GR/C/62871.
- [11] Evaluation of the Solar Reflectance of Four Samples of Painted Cement submitted for test by Cardiff University Industry Centre. B M Cross. February 1986. EETS Ref no. 2.
- [12] Sikkens, Permoglaze, Sandtex: Trade Colour Card. 1992. AKZO Coatings plc.
- [13] British Standard 4800. Paint Colours. British Standards Institution.
- [14] Colour Dimensions. ICI Paints Ltd.
- [15] Dow Chemicals. Styrofoam for Cold Storage Insulation. February 1989.
- [16] British Standard 874 Part 2: Section 2.1. Methods for determining thermal insulating Properties. British Standards Institution.
- [17] Rockwool product information

APPENDIX 1 - Calculation of corrections for thermal edge effects

Some aspects of structure heat losses in the EMC Test Cells at Cranfield

A.G. Guy
(Pilkington R&D Laboratories, Lathom, Lancs)

Introduction

At a previous discussion concerning the Test Cell studies being carried out by EMC at Cranfield (ETSU group meeting, Cranfield, 29th Oct. 87), it was observed that average overall heat loss coefficients measured for the cells were somewhat higher (typically c10%) than those indicated by simple calculation. One possible factor suggested as contributing to this was that calculated overall structural heat loss characteristics were built up by summing individual component 'UxA' contributions with the 'A's being defined on an internal surface basis only. Thus, edge and corner effects were essentially ignored.

For simple structures of uniform properties and reasonable geometries, analytic solutions or approximations can often be used to relate such edge heat flow effects to a suitable level of accuracy, at least on a two dimensional basis (e.g. Ref.1 , chp.16). These latter are usually sufficiently satisfactory for the required purpose. In the EMC test cells, however, structural aspects are not quite so simple, particularly around edges of walls, etc., and analytic approaches for evaluating edge heat flow effects do not seem practical.

While analytic procedures may not be suitable, problems such as this can be readily tackled using numerical computation. This brief note provides several examples of computational application to typical edge structures occurring in the EMC test cells. Hopefully, these may provide useful information for future examination and discussion.

Test cell structure aspects

Within the scope of this note, it is not possible to cover many examples. The applications considered here relate to Fig.2.1 of Ref.2 (reproduced as Fig.1 of this note for convenience). On the basis of this, the following assumptions are made.

- (a) A 'base' representative test cell external wall structure (for comparative purposes only, outside to in, see Fig.1, and rounding some dimensions where appropriate for convenience) consists of
 - Outer ply (13mm)
 - 100mm glass fibre between 100x35mm studs at 400mm centres
 - 25mm air gap
 - Inner plasterboard (13mm)
- (b) Thermal properties of the various component materials are as given in Table 2.2 of Ref.2, those relevant for this note being as follows.

<u>Material</u>	<u>Thermal Conductivity (W/mK)</u>
External ply	0.181
Glass fibre	0.043
Softwood	0.125
Plasterboard	0.15
Hardboard	0.11

- (c) Representative surface resistances of $0.12\text{m}^2\text{K/W}$ and $0.06\text{m}^2\text{K/W}$ apply for interior and exterior surfaces respectively.
- (d) The equivalent conductivity for the 25mm air gap corresponds to a gap thermal resistance of $0.18\text{m}^2\text{K/W}$ perpendicular to the plane of the wall.

Representative wall structure properties

It is to be expected that one dimensional approximation of thermal properties on a bridged proportional area basis (e.g. Ref.3) is likely to prove fairly reasonable for an infinitely repeating 'base' wall structure as represented by (a) above. Taking a minimum representative section of 200mm width (i.e. between centre lines of stud and insulation), with other assumptions as above, then the calculated heat exchange coefficient H, per unit length of such section following Ref.3

$$H, = 0.0784 \text{ W/K per m length.} \quad (1)$$

For comparison, an equivalent computational analysis of the same problem yields the result

$$H, = 0.0790 \text{ W/K per m length,} \quad (2)$$

i.e. an increase of less than 1% on the much more simply obtained conventional empirical calculation. (This is not surprising, since the empiricism of Ref.3 has essentially been formulated on the basis of many similar comparisons.)

It can be inferred therefore that as far as non-uniform structures not containing edges and corners are concerned, the conventional empirical methods of calculation should be satisfactory for evaluating average heat loss coefficients (probably to around the 1% level for the test cells).

Examples of edge heat flow behaviour

Two cases are considered here, both based on Fig.1 , as follows.

Example 1: Vertical wholly exposed northerly edge structure (ringed 'A' on Fig.1).

Computer analysis of this example was carried out, again using the assumptions outlined above as appropriate. Fig.2 illustrates predicted temperature isotherm behaviour (one tenth ΔT intervals) in the region of the edge corner and extending into the more uniform regions of structure away from the edge junction where heat flows become essentially one dimensional. At the edge corner however, internal

surface temperatures are lower than those away from the edge (by around 10% of the internal to external temperature difference), implying a higher localised cooling effect at the edge junction.

To attempt to provide quantitative interpretation of the influence of the edge heat flows, for convenience here they will be referenced to the 'representative' heat exchange behaviour above (though this will presumably differ from the practical reference applied by EMC). It is therefore convenient to consider an edge junction that extends to 200mm from the edge corner line on both wall internal surfaces (see e.g. Fig.2). The 'representative' structure heat loss coefficient H_1 , for this extent of surface would be (from (2), x2 for 400mm)

$$H_1 = 0.158 \text{ W/K per m length. } \quad (3)$$

The corresponding structure heat loss coefficient H_1 , for the same configuration as calculated from the computed results is

$$H_1 = 0.202 \text{ W/K per m length,} \quad (4)$$

i.e. some 28% higher than the above.

For practical purposes, however, the scale of influence of the edge effect would need to be assessed by determining the additional loss coefficient contribution for the whole length of edge. As a guide to how significant this can be, consider a hypothetical isolated enclosure of appropriate 'representative' structure as above of internal dimensions 2x2x1.6m (hxdxw, i.e. not too dissimilar from those of the test cells). An overall heat loss coefficient H_E for such a structure based on representative properties would be around (overall internal surface area $2 \times 4 + 4 \times 3.2 = 20.8 \text{ m}^2$)

$$H_E = 8.2 \text{ W/K.} \quad (5)$$

Assuming 4 vertical edges (each 2m length) of the type considered above would be expected to produce an additional contribution ΔH_E to the heat loss coefficient of $(4 \times 2 \times (.202 - .158))$

$$\Delta H_E = 0.35 \text{ W/K,} \quad (6)$$

i.e. an increase of around 4-5%. With a further 8 horizontal edges still to be taken account of (though these would usually be of different configuration), it is easy to see that heat loss coefficients calculated on simplified 'UA' bases can readily be underestimated by of the order of 10% or so if edge effects are ignored. This may help to account for at least some the apparent observed underestimation for the EMC cells.

Note: Such underestimations will become relatively more significant as enclosure size decreases, and as wall thicknesses and insulating properties increase.

Example 2: Vertical north edge at dividing wall between rooms 2 and 3 (ringed 'B' on Fig.1).

This was analysed computationally in similar manner to example 1 above. For the analysis, it was assumed that the internal conditions in rooms 2 and 3 were identical, so that the central plane of the dividing wall was a 'no flux' boundary, with temperature behaviour symmetric about this. Fig.3 illustrates the computed temperature isotherms in analogous fashion to those of example 1 (Fig.2).

If edge heat loss behaviour is again referenced to a 'representative' level, though this time to a 200mm section (i.e. northerly facing only, the losses through the dividing wall assumed to have been taken as zero in a conventional approach), then the different heat loss coefficient contributions would be as follows (cf example 1).

'Representative'	0.079W/K per m length,
Computed	0.109W/K per m length.

This increase is greater in relative terms (though less in absolute) than that observed with example 1. It can be expected to contribute in similar manner to overall heat loss coefficient behaviour.

Other specific examples pertaining to the EMC test cell structures could be similarly analysed. However, further computations are beyond the scope of this note, the purpose of which is to attempt to illustrate some behaviour of edge heat flows, and give an intuitive idea of the influence that these can have on structure heat loss coefficients.

It would be advisable for EMC to assess the above observations in relation to their own procedures for estimation of cell overall heat loss coefficients. In the longer term, it may be possible to extract adequate empirical rules/guidelines for dealing with edges and/or corners. At the moment, however, computational approaches seem satisfactory, albeit at the expense of being more time consuming and complex.

Inferences

Some inferences which may be drawn are as follows.

- (a) Empirical rules for evaluating structure heat loss properties (e.g. Ref.3) should be sufficiently satisfactory for regions where corner or edge effects are not relevant.
- (b) If edge/corner effects are not fully taken into account when calculating overall heat loss coefficients for enclosures, some underestimation of these latter will result. This may explain at least part of the discrepancy observed for the EMC test cells. EMC should examine the restricted examples provided here with a view to providing further comment on this.

- (c) Computational procedures currently provide a means of evaluating overall heat loss coefficients more accurately than conventional empirical calculations, though at the expense of added complexity.


.....
A.G. Guy, /Jan. 1988

References

- | | |
|----------------------------------|---|
| 1. Carslaw, H.S., & Jaeger, J.C. | "Conduction of Heat in Solids"
Oxford UP (1959) |
| 2. Energy Monitoring Company | "Test Cell Studies 1",
ETSU S-1162 (1987) |
| 3. CIBSE | Guide A3, "Thermal Properties
of Building Structures" (1980) |

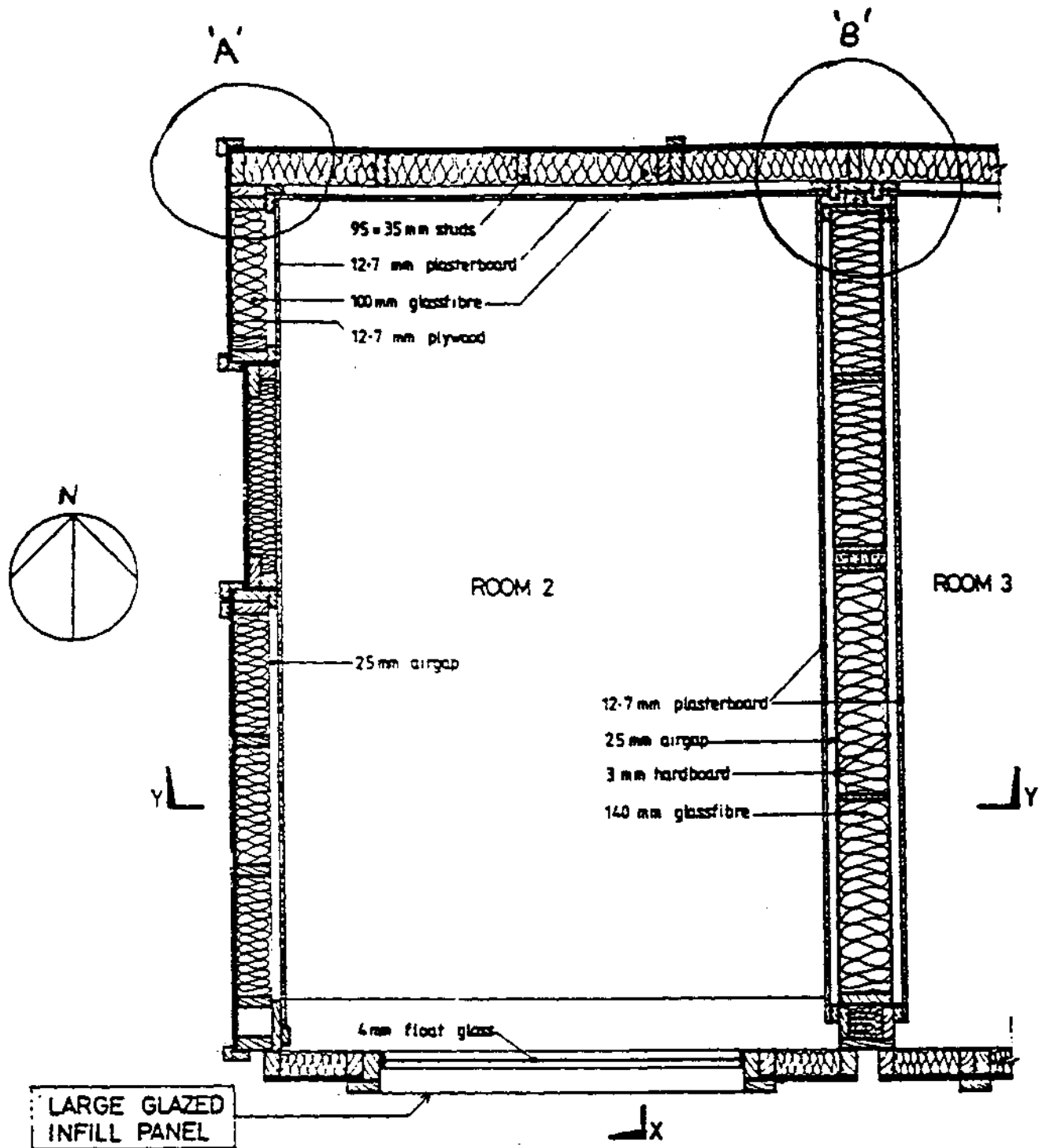


Fig. 1: Plan view of EMC test cell

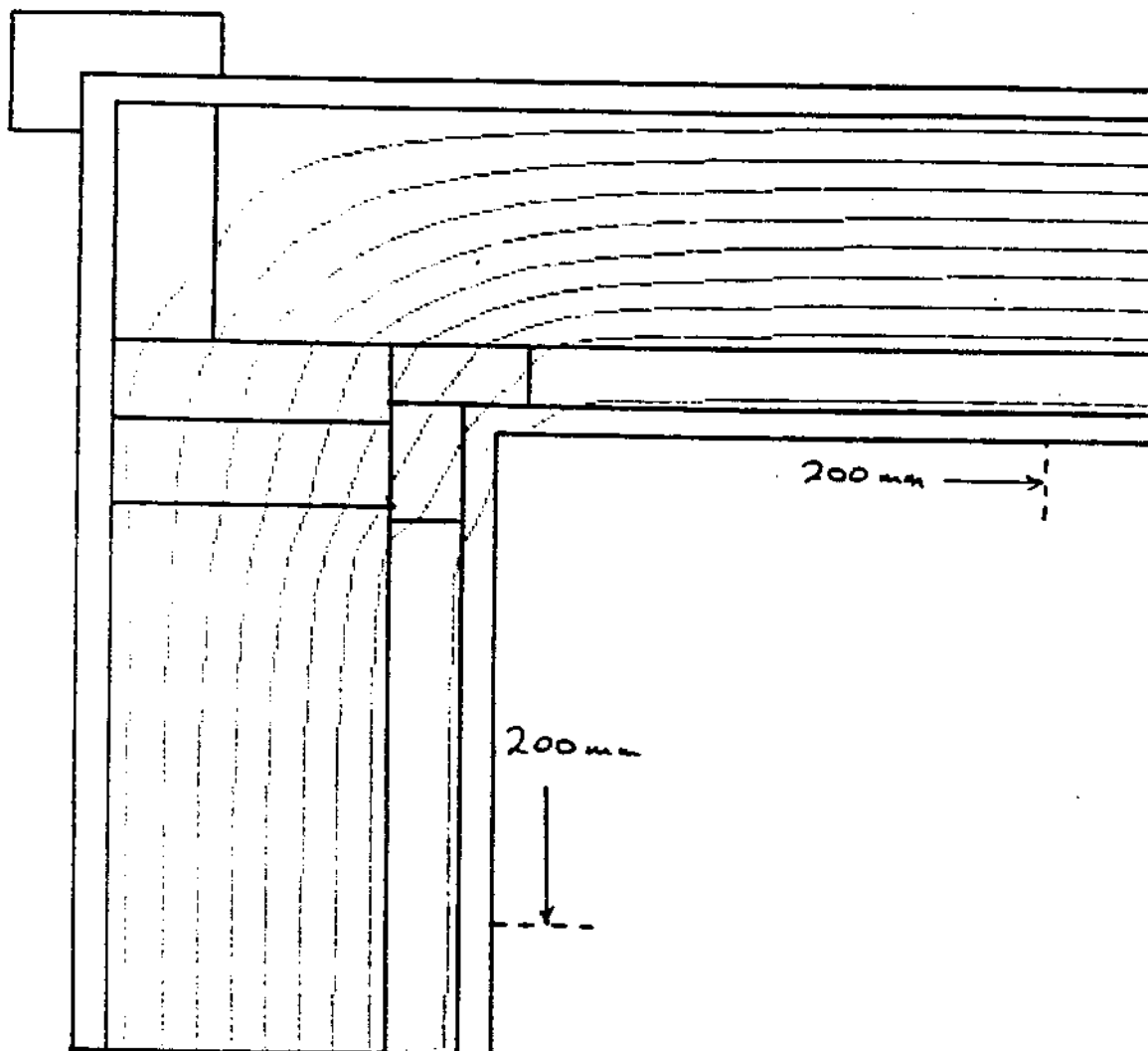


Fig. 2: External edge corner isotherms

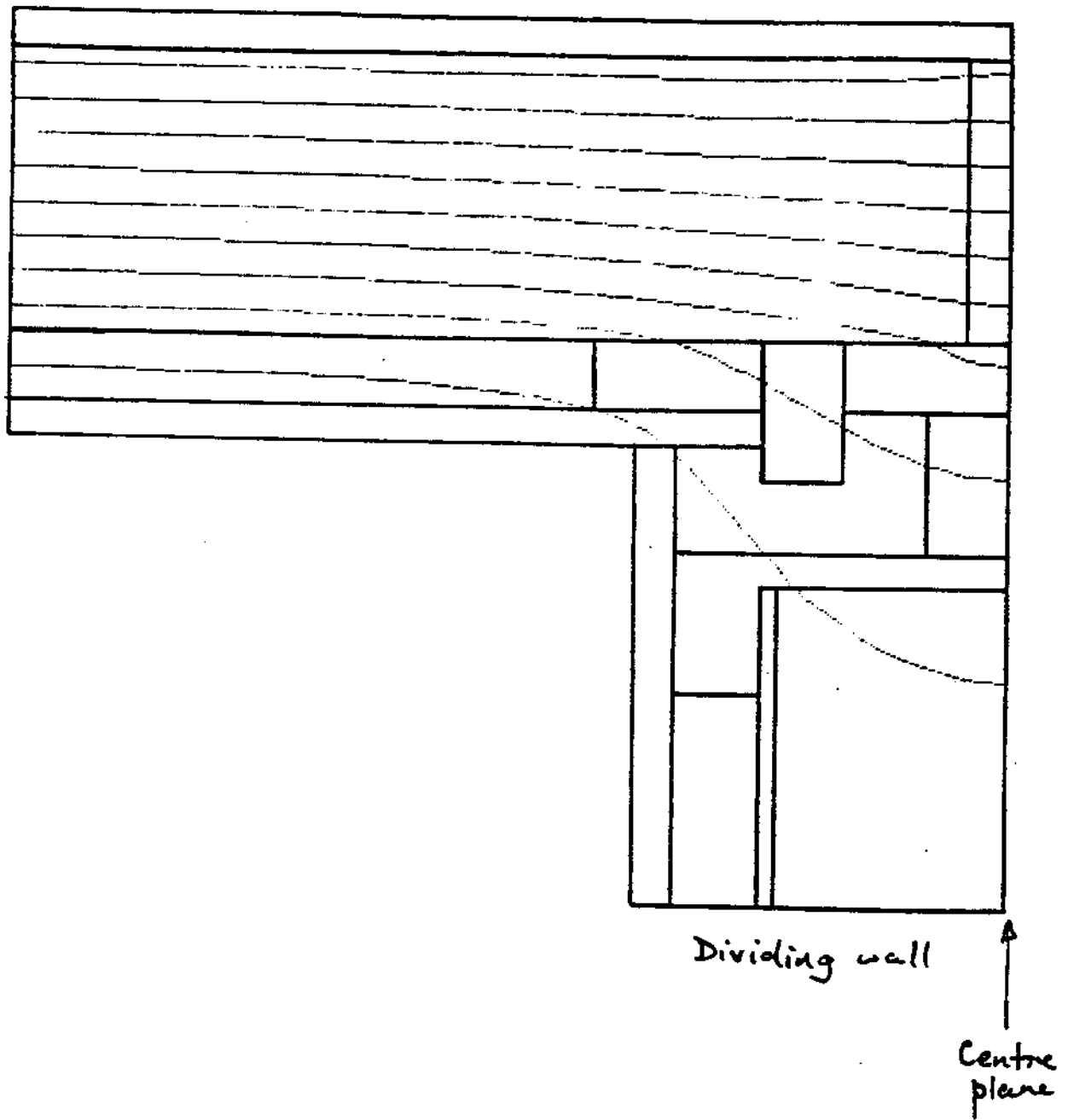


Fig.3: Dividing wall isotherms

Calculation of increased heat loss due to edge effects in the EMC test rooms and its incorporation into SERI-RES and HTB2

Consideration of the geometry of the test room construction suggested that the increase in heat loss through the ceiling and floor due to edge effects was likely to be small. Effects around the party wall to the adjacent cell were similarly ignored. Thus only the North, external side and South walls were considered. Table 1 shows the total loss through the 200mm wide edge region of each of these surfaces. The table also shows the edge loss implicit in the building description which Leicester Polytechnic had used to carry out the earlier experimental design simulations. The increase in heat loss through each surface is then readily available as the difference between these figures.

Table 1 - Estimation of increased heat loss due to edge effects

	North	Ext	South	
1 Type A edge strip heat loss	0.101	0.101	0.101	W/mK
2 Type B edge strip heat loss	0.109	0.109	0.109	W/mK
3 Length of type A edge	2.278	4.556	2.278	m
4 Length of type B edge	4.878	4.300	4.878	m
5 Total edge heat loss (1*3)+(2*4)	0.762	0.929	0.762	W/K
6 Typical existing edge loss	0.070	0.070	0.070	W/mK
7 Total edge length (3+4)	7.156	8.856	7.156	m
8 Existing total edge loss (6*7)	0.501	0.620	0.501	W/K
9 Increase in heat loss (5-8)	0.261	0.309	0.261	W/K

Table 2 shows how the k-values of the framing timber were modified to achieve these increased heat losses. The UA-value of the framing surfaces in the building description used by Leicester at the experimental design stage is calculated. Then the heat loss required is obtained by adding in the extra losses determined in table 1. From this the new frame U-value required is calculated.

The modified k-value required for the timber is then calculated by first finding the U-value of the remaining components of the frame, by subtracting the original timber U-value from that of the old frame section. Then the contribution required to the frame U-value from the modified timber can be calculated. From this, the k-value of the modified timber follows directly.

Table 2 - Modification of framing timber k-values to account for increased edge heat losses

	North	Ext	South	
Frame construction code	C15	C15	C02	
10 U-value of old frame construction	0.782	0.782	0.943	W/m ² K
11 Area of frame	0.367	0.918	0.578	m ²
12 UA-value of old frame (10*11)	0.287	0.718	0.545	W/K
13 UA-value required (9+12)	0.548	1.027	0.806	W/K
14 Frame U-value required (13/11)	1.493	1.119	1.394	W/m ² K
Material code of timber in surface	W95	W95	W110	
15 k-value of timber	0.125	0.125	0.125	W/mK
16 Thickness timber in construction	0.095	0.095	0.110	m
17 Timber U-value (15/16)	1.316	1.316	1.136	W/m ² K
18 U-value of old frame less timber 1/(1/10-1/17)	1.928	1.928	5.542	W/m ² K
19 U-value required from new timber 1/(1/14-1/18)	6.618	2.665	1.863	W/m ² K
20 Revised timber k value (19*16)	0.629	0.253	0.205	W/mK

Finally, table 3 summarises the new, fictitious, framing timbers which were introduced into the test room building description.

Table 3 - New framing materials to account for edge effects

Material code	Used in surface	k-value
W95A	North wall	0.629 W/mK
W95B	External wall	0.253 W/mK
W110A	South wall	0.205 W/mK

APPENDIX 2 - Distribution of solar radiation entering glazed test rooms

Element	Fraction of incoming solar radiation
Solar lost back to exterior by shortwave reflection	0.20
Solar communicated directly to room air	0.05
Floor	0.29
South wall (glazing surround)	0.04
West wall	0.12
East wall	0.12
North wall	0.09
Ceiling	0.09
TOTAL	1.00

Table A2.1: Distribution of solar radiation entering test rooms with 1.5m² glazing

Element	Fraction of incoming solar radiation
Solar lost back to exterior by shortwave reflection	0.11
Solar communicated directly to room air	0.05
Floor	0.31
North wall	0.09
West wall	0.14
East wall	0.14
South wall (glazing surround)	0.06
Ceiling	0.10
TOTAL	1.00

Table A2.2: Distribution of solar radiation entering test rooms with 0.75m² glazing

APPENDIX 3 - Timing of weather data supplied

IEA Task 21: Timing of weather data supplied for validation exercise

1 The problem

The weather data supplied for this exercise consists of average values accumulated over the course of each hour, that is from $x:00$ to $(x + 1):00$. At EMC this value would be labelled with hour number $x + 1$. Data thus refers to the hour preceding the point at which it is recorded, a convenient assumption when that data is being gathered in real time. This is the convention normally used in the US.

In the UK, however, met. data is generally averaged from one half-hour point to the next, ie from $(x-1):30$ to $x:30$. Such a value will normally be labelled with hour number x , as it is centred on $x:00$.

A query has arisen about the use of the data as supplied with certain UK programs, most notably ESP, which requires data in the UK format.

2 Background

The data sets being used in this exercise were originally gathered for use in two ETSU validation projects in which SERI-RES was to be tested. SERI-RES has been modified to accept data recorded to the UK convention, but the modification was not comprehensive and introduced a series of bugs into the program. Accordingly, the modification was removed from the EMC copy of the model, and weather data in the US format is always used.

Of the two data sets currently being used, v099 was constructed from five minutely data, and a version of that data can thus be constructed using the UK timing convention.

The data in v 110, however, was averaged on the site data acquisition system and then recorded at hourly intervals. In this case the UK version of the data is not directly available.

Previous sensitivity studies have indicated that, in one particular configuration, changing data type caused a 4% change in predicted energy consumption. It is therefore clear that something should be done about the problem.

3 A solution

One (approximate) solution to this problem is to use a moving average filter (MAF) to correct the US data, that is the required average value between $(x-1):30$ and $x:30$ is approximated by:

$$D_{(x-1):30 \rightarrow x:30} \approx \frac{1}{2} [D_{(x-1):00 \rightarrow x:00} + D_{x:00 \rightarrow (x+1):00}]$$

This solution is, however, only an approximation to the required information. In particular, the averaging process is likely to 'smooth' *any* high frequency fluctuations in the data.

4 Data disk

The files on the attached disk are described in the table below.

Filename	Contents	First line hour number	First line averaging period
v099.met v110.met	Original (US format) data files	1	0.00 → 1:00 am
v099.smt v110.smt	Data files adjusted to UK format using MAF	0	23:30 → 0.30 am
v099.emt	Data file built to UK format from recorded data	0	23:30 → 0:30 am

The attached graphs, all plotted starting from the first line in the v099 data files, show the effects of using the MAF and of building the data from the measured results. Points to note are:

- for ambient temperature, which is a slow moving quantity and therefore immune to further smoothing, the MAF gives good results,
- on the first day, which is clear, the MAF provides good results on solar radiation data except at noon when there is a momentary error as the curve changes direction, and

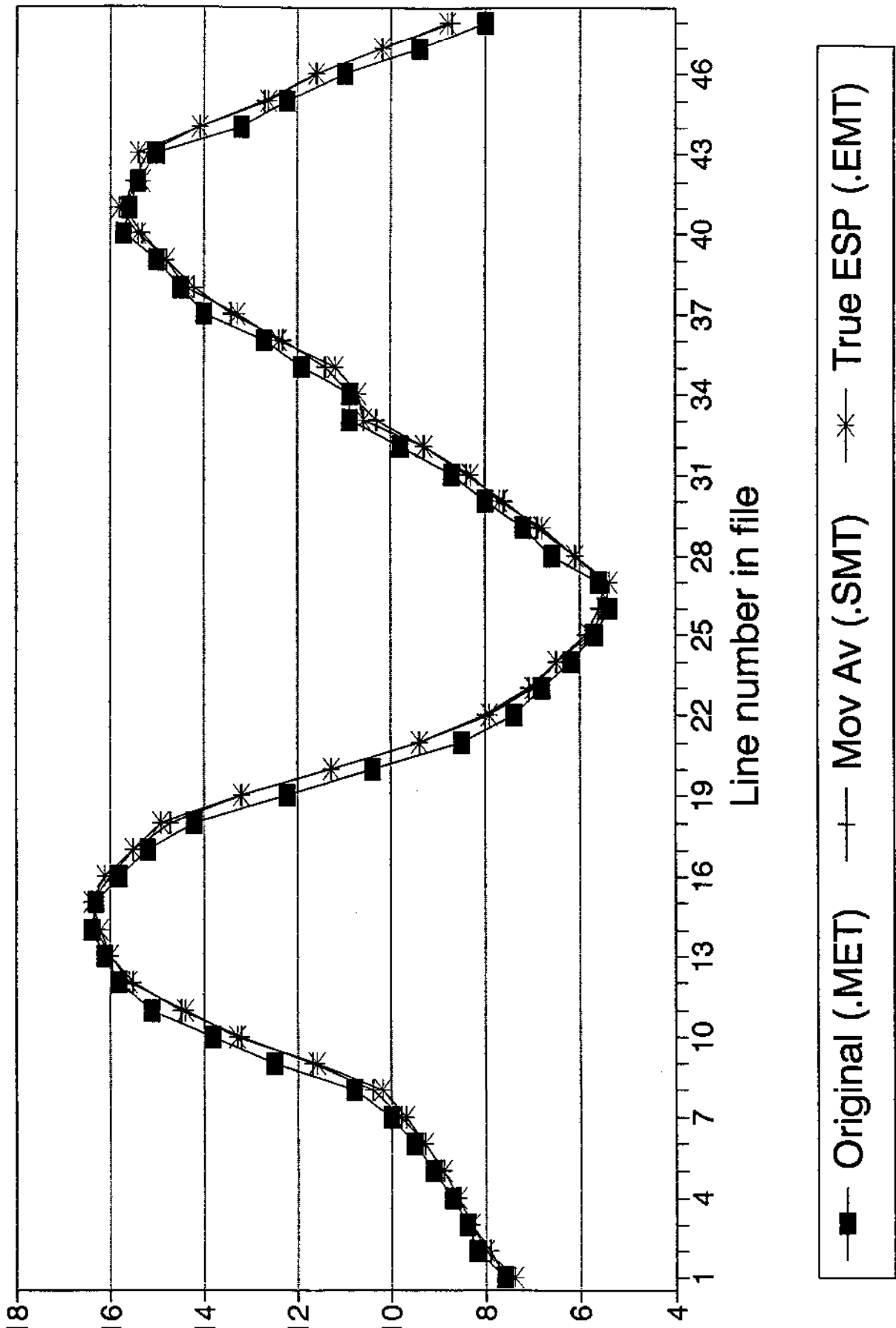
on the second day, when variable cloud cover has caused some fluctuations in radiation level, the MAF gives poorer performance due to the smoothing effect described earlier. Even so, a large amount of the potential 4% difference will have been corrected.

5 Conclusions

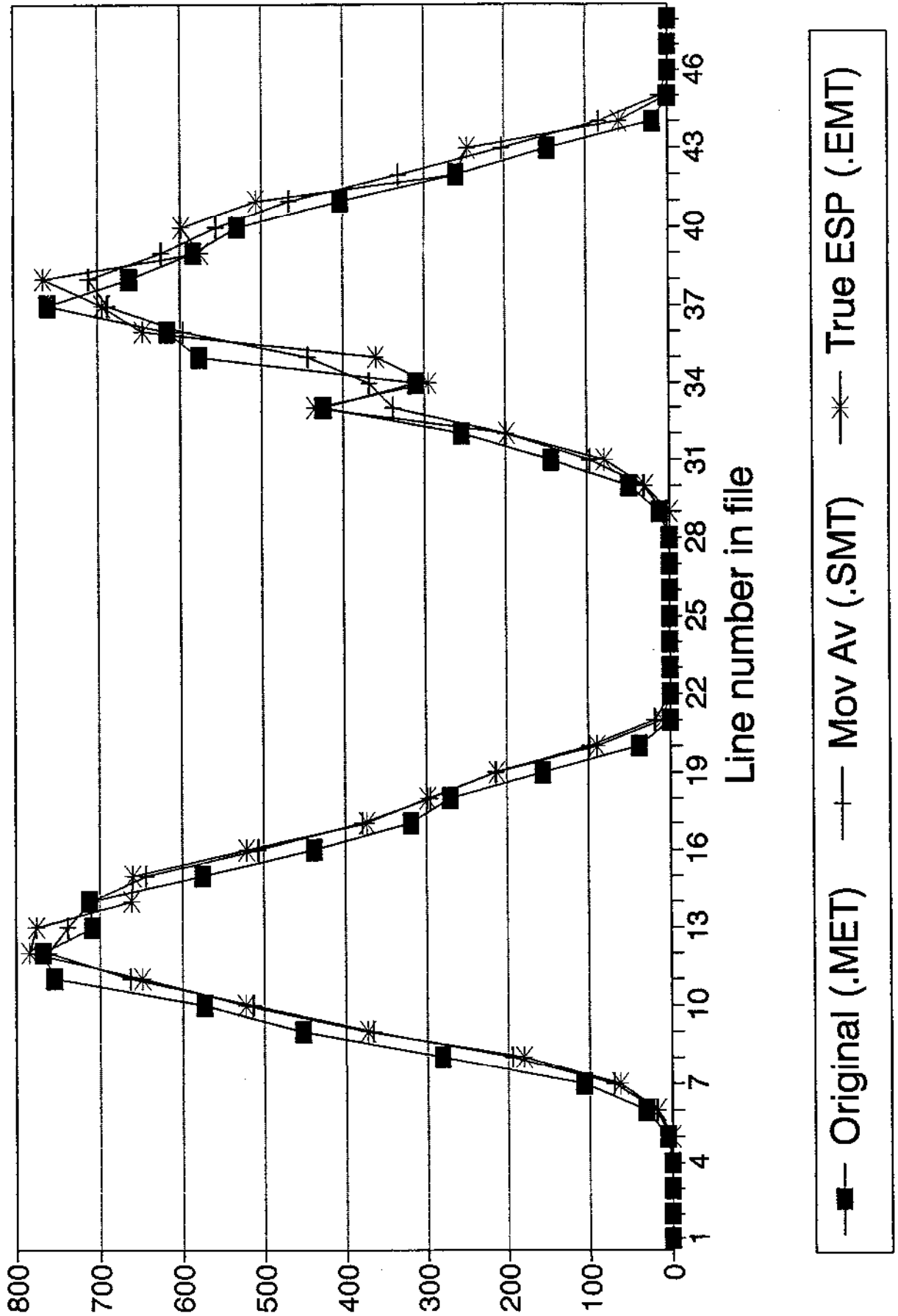
Data sets 'corrected' using the MAF have been supplied for both periods. A data set averaged from the original data has been provided for one of those periods. Initial qualitative comparisons indicate that the MAF performs acceptably. If there are further concerns these may be resolved by performing a sensitivity study using the MAF and correctly averaged data sets.

Alternative met data for use with ESP

Ambient temperature



Alternative met data for use with ESP Global horizontal radiation



CONTENTS

1. Introduction
2. Phase 1: Blind
 - 2.1 Recommended Procedure
 - 2.2 Modelling the Rooms
 - 2.3 Digital Outputs
3. Phase 2: Non-blind

REFERENCES

1. INTRODUCTION

This guide was originally produced for subtask C (Model Evaluation) of International Energy Agency, Annex 21 (Calculation of Energy and Environmental Performance of Buildings), which worked jointly with Subtask B of Task 12 (Building Energy Analysis and Design Tools for Solar Applications). It has since been updated and is to be used in conjunction with Part 1 of this Validation Package, the Site Handbook, and Part 4, the Data Disk. It describes a process for evaluating the predictions of thermal programs of buildings.

The field measurements are of very high quality, so the data sets have minimum uncertainty associated with them. This empirical validation tool therefore has the potential to closely discriminate between those programs which are performing well and those which are not.

Although the actual measured performance data for the test rooms is supplied on the associated Data Disk, users of the Validation Package are strongly advised to firstly carry out their simulations 'blind', i.e. without knowledge of the measurements. The aim is to mimic the conditions which exist when a program is used to predict the performance of an actual building. It should be noted that a conscious decision has been made to include only fundamental physical properties of the test cells in the Site Handbook. This means that other information which is required by some programs (because of the simplifying assumptions they make about certain physical processes) is not included. Examples are surface coefficients and window U-value.

Having undertaken the first 'blind phase', a second phase may be undertaken to explore the differences between the program predictions and the measured data.

2. PHASE 1 : BLIND

2.1 Recommended Procedure

In all, six sets of hourly results can be analysed, one for each of the three rooms for both weather volume 099 and weather volume 110 (Table 1).

Weather Period	Room	Glazing Type	Glazing Area	Heating	Suggested Results File name
099	Room 1	Double	1.5m ²	None	fd.res
099	Room 3	Opaque	-	None	fo.res
099	Room 5	Single	1.5m ²	None	fs.res
110	Room 1	Double	1.5m ²	Heated 06:00 - 18:00	hd.res
110	Room 3	Opaque	-	Heated 06:00 - 18:00	ho.res
110	Room 5	Double	0.75m ²	Heated 06:00 - 18:00	hs.res

Table 1 Weather periods and room descriptions

Once sets of results have been obtained 'blind' using the basic parameter values listed in Part 1, Site Handbook, they should not be altered. It is therefore wise to proceed cautiously using the program to

be validated as accurately as it allows. The following steps could be followed.

- A. Check that the Disk, Site Handbook and this Guide are complete.
- B. Read this Validation Guide and the Site Handbook completely before beginning work.
- C. Load the weather data off the disk onto the local computer.
- D. Plot the two 10-day weather sets and check that the data reproduces the graphs in the Site Handbook (Figs. 7.1 to 7.6).
- E. Reformat and convert the weather files as necessary to create the files needed by the prediction program. Take care to use the correct timing conventions (Appendix 3 of the Site Handbook). Replot the data and check for spurious values (particularly of solar irradiance).
- F. Model each of the Rooms in as much detail as the simulation program will allow. Avoid any unnecessary approximations (see section 2.2).
- G. Configure the program as necessary to generate the five or six hourly outputs required for each room and weather combination (see section 2.3).
- H. Conduct the six ten-day simulations and save the output for the last seven days of each one.
- I. Undertake any averaging or totalling necessary to produce hourly outputs, and convert these into the format given below (Tables 2 to 4).

2.2 Modelling the Rooms

The following points should be noted when modelling the rooms.

- A. Model both the room and the roofspace.
- B. It is unnecessary to model the shading effects due to the glass being recessed by 10mm. Site shading due to adjacent rooms may be important.
- C. Avoid reflected solar radiation impinging on the underside of each test room floor - this does not happen in practice.
- D. Explicitly model each and every construction in each surface.
- E. Take care when modelling the "adiabatic" party wall (see Part 1, Site Handbook section 5.1, Table 5.6).
- F. Derive any glazing transmission properties from the fundamental properties for a single sheet (given in Table 5.9 of the Site Handbook).
- G. Model the distribution of solar radiation as accurately as possible (see Site Handbook, Appendix 2 if guidance is needed).

- H. Assume that there is no infiltration into the test rooms, assume one airchange per hour in the roof space (see Site Handbook, section 5.4).
- I. Model the radiant/convective split of the heater, its time constant and any other aspects (physical size, location) as accurately as possible (section 5.4 of the Site Handbook).

2.3 Digital Outputs

For each of the six room and weather combinations, five or six parameters should be predicted for each of the 168 (7 x 24) hours of the comparison period.

- A. The hourly external south-facing, vertical, global solar irradiance, which should be the total of both the direct and the ground reflected parts.
- B. The hourly heating energy consumption for weather volume 110 only.
- C. The mean hourly space air temperature.
- D. The mean hourly inside surface temperature of the floor (construction C37).
- E. The mean hourly inside surface temperature of the back wall (construction C 16).
- F. The mean hourly inside surface temperature of the ceiling (construction C 11).

It is recommended that one results file should be produced for each data set. Each of these will be 171 lines long and in the format shown in Tables 2 and 3. This format can be generated using the write statements given in Table 4. It is the same format as the data disk containing the measurements (Part 4 of this validation package), and will therefore make comparisons easier.

3. PHASE 2 : NON-BLIND

The purpose of this phase is to explore, and hopefully discover, the reasons for any mismatches between the measurements and the predictions of the program. This is likely to be a loosely structured process. Exploration procedures and the associated statistical techniques for diagnosing simulation errors are still active areas of research. Nevertheless, it is hoped that the following suggestions will be helpful.

- A. Firstly, if the predictions made in the blind phase differ significantly from the measurements, check for errors in the model input files. This may indicate an area of ambiguity in the program manual, or user interface. Possible improvements to these, and any necessary refinements to in-house quality assurance procedures, should be considered.
- B. Having corrected obvious errors re-run the simulation program and compare the results with measurements at both the hourly level and using the aggregated 7-day energy totals and maximum and minimum temperature values. Detailed measurements are on the data disk to assist in this process.
- C. To test whether any discrepancies between the measurements and predictions are due to experimental errors or program inaccuracies, sensitivity analysis should be undertaken. To permit

this, the uncertainty on all the important parameters used in most thermal programs have been listed in the Site Handbook.

There are two useful techniques, Monte-Carlo Analysis or Differential Sensitivity Analysis, both will provide similar estimates of the experimental error. These should be combined (in quadrature) with the measurement uncertainty (Table 6.1 of Site Handbook) to produce an overall 'error bar' which can be placed around the measured results (hourly trace or 7-day totals). If the predictions lie outside this error band it indicates that there is a 95% chance that errors remain in the simulation results. An example of this procedure can be found in Reference 1^[1].

- D. If errors are found in the program then diagnostic tests are needed to uncover these. The measured data alone may offer clues. For example, the solar processing can be checked using the measured south facing vertical solar irradiances. The variation with time of the air temperature or power consumption may suggest errors in heater or thermostat modelling.

Other approaches to diagnosis would include algorithmic substitution, to test whether the predictive accuracy improves when alternative (more sophisticated) approaches for modelling the same thermal process are adopted. It may also be possible to utilise advanced cross-correlation or time-series analysis to identify the cause of any observed errors.

Looking beyond this empirical validation study, a series of building energy simulation tests (BESTEST) were developed as part of the IEA Task 12/Annex 21 exercise. These succeeded in revealing errors in all the major simulation programs which participated in the TEA study. The use of these tests will require further building modelling. The BESTEST document explains fully how to undertake the tests and how to interpret the results.

REFERENCES

1. Lomas, K.J., Eppel, H., Martin, C. & Bloomfield, D., International Energy Agency Annex 21C/Task 12B, Empirical Validation of Detailed Thermal Programs using Test Room Data, Volume 1: Final Report, IEARR6/93, Nov. 1993
2. Judkoff, R. & Neymark, J., Building Energy Simulation Test (BESTEST) and Diagnostic Method, Report of IEA Task 12B/Annex 21C.

Room R Volume VVV

```

=====
DDD HH IIII KKKKKK AAA.AA FFF.FF WWW.WW CCC.CC
|   |   |   |   |   |   |   |   |
|   |   |   |   |   |   |   |   |
=====
DDD HH IIII KKKKKK AAA.AA FFF.FF WWW.WW CCC.CC
=====

```

Table 2 Layout of Data Entries for Each Data Set

Item	Entry	Units	Examples	Type	Notes
R	Room Number	-	3	I1	Room Number
VVV	Volume Number	-	099	I3	Weather Volume
DDD	Day Number	-	147	I3	As data diskette
HH	Hour Number	-	16	I2	Hour 01 = 00:00 to 01:00 etc.
IIII	External South Facing Vertical Solar Irradiance in Plane of Glass	Wm ⁻²	1245	I4	Total of direct and ground reflected components
KKKKKK	Hourly Energy Use	KJ	000054	I6	Total during the hour (110 only)
AAA.AA	Temperature of room air	°C	38.72	F6.2	Spatial average temperature
FFF.FF	Temperature of floor	°C	23.76	F6.2	Inner surface of construction C37
WWW.WW	Temperature of wall	°C	17.62	F6.2	Inner surface of construction C16 (north wall)
CCC.CC	Temperature of ceiling	°C	15.39	F6.2	Inner surface of construction C11

Table 3 Data Items Required for Each Data Set

Line	Format	No. Characters
1	"ROOM", IX, I1, 2X, "VOLUME", 1X, I3	18
2	46 ("=")	46
3-170	I3, 1X, I2, 1X, I4, 1X, I6, 4(1X, F6.2)	46
171	46 ("=")	46

Table 4 Format of Results for Each Data Set

CONTENTS

	page
1 INTRODUCTION	1
2 CONSTRUCTION OF THE TEST ROOMS	1
2.1 Initial construction	1
2.2 Deterioration with time	2
2.3 Airtightness	2
2.4 Post-operation checks (decommissioning)	4
2.5 Site location	5
3 MATERIAL PROPERTIES	6
3.1 Insulation materials	6
3.2 Thermally massive materials	6
3.3 Opaque surface properties	7
3.4 Glazing	7
4 INSTRUMENTATION	7
4.1 Temperature	7
4.2 Solar radiation	7
4.3 Electrical power	8
5 ESTABLISHING MATCHING BETWEEN PAIRS OF TEST ROOMS	8

REFERENCES

FIGURES

1 INTRODUCTION

The Energy Monitoring Company (EMC) has, for the past seven years, operated an outdoor test site which now comprises a total of ten test rooms. The site and the test buildings are described in detail in [1] and [2]. Over that period data have been gathered from the rooms for component testing, determining parameters for input to simulation models and for empirical model validation.

In this latter application data from the test rooms have been compared with the simulation program SERI-RES in a two year project to determine the accuracy available from that code [3]. More recently data from the test rooms have been used to carry out empirical model validation as part of LEA Annex 21C/Task 12B. In this project data from the test rooms were compared with the predictions of 25 different program/user combinations [4] from Europe, North America and Australia.

The applications described require that the data produced in the test rooms be of the highest quality. It could be argued that model validation is the most critical application - data which have large uncertainties associated with them will result in a very weak test of any model. More seriously, data which are actually incorrect, that is for which the true values lie outside the confidence intervals associated with the measurements, may result in erroneous conclusions. A model which works satisfactorily may be rejected on the grounds of such erroneous measurements or, even more seriously, a model which contains errors may be deemed to function correctly.

This report describes the measures which have been taken to ensure that data from the EMC site are consistently of the highest quality. The problem of ensuring data quality is divided into three areas:

- the way in which the test rooms are constructed must be known,
- the properties of the materials used must be known, and
- the instrumentation used to measure climate and the performance of the rooms must be accurate.

Ensuring quality in each of these respects consists of two parts: determining that the initial installation is of high quality, and ensuring that the equipment remains serviceable throughout its operating life, that is that the system properties do not drift.

The remainder of this document describes how each of these requirements is addressed at the EMC test site. Section 2 describes the measures taken to ensure that the construction of the test rooms is well known and consistent. Section 3 describes the measures taken to ensure that the properties of the materials are well known. Section 4 describes the controls applied to the site instrumentation. Finally Section 5 briefly outlines a method which has been developed to establish the degree of matching between the test rooms, and discusses its role in the quality assurance process.

Quality assurance is of necessity a progressive process, being refined over time in response to faults which are found within instrumentation or buildings. The procedures discussed in this short document summarise the developments which we have made in this field over the past seven years. We fully intend to continue to improve these procedures, and with this aim in mind any comments or criticisms on this report will be most welcome.

2 CONSTRUCTION OF THE TEST ROOMS

2.1 Initial construction

Establishing whether the initial construction of the test rooms is as intended relies on the attention to detail and diligence of the person carrying out construction tasks. However, there are several measures

which can be used to ensure that this work is as accurate and consistent as possible:

- individual tasks are undertaken by a single person, who takes responsibility for that task from start to finish. This prevents errors creeping in when one member of the team erroneously believes that another has completed part of a given task,
- whenever possible EMC avoids the use of external sub-contractors. This avoids the difficulty of ensuring that such contractors carry out the work exactly as required, and it also avoids mistakes which could occur when individuals not familiar with the ultimate use of the structures carry out work on them. One example of this, resulting from the use of an external glazing contractor, will be described later in this report. Finally,
- in order to ensure that no step in the construction process is missed check lists of all the tasks which must be carried out in the construction of the rooms are extensively used. In this way it is much less likely that something will be overlooked. This approach is particularly valuable when a number of identical buildings are being constructed at the same time, when a task could easily be overlooked in one room.

2.2 Deterioration with time

Continuous checks are necessary to determine that long term deterioration of materials and construction is not taking place. Attention to the issue of deterioration at the design stage can greatly reduce long term problems, and *can* greatly simplify the checking process. For example:

- careful detailing (particularly underneath the rooms) can ensure that no damage is caused by rodents or insects,

careful detailing must be used to ensure that water does not penetrate the parts of the structure which influence the thermal performance of the rooms. For example, butt joints should not be used in the outside skin of the rooms, as water will eventually penetrate by capillary action. Joints which rely on mastic to make a waterproof seal should also be avoided, as they will eventually crack due to the movement which is inevitable in any building sized structure,

- the construction should be such that if water ingress does occur it can be readily detected and its effects remedied. An accessible roofspace is one way of achieving this for the most likely source of leaks, the roof,

materials which do not absorb moisture should be used wherever possible. This will limit the damage in the event of a sudden ingress of water, and will also avoid longer term variation in properties due to the absorption of atmospheric moisture,

materials whose properties degrade with time due to, for example, outgassing should be avoided. In the EMC test rooms polyurethane foam is used only to seal small gaps to minimise infiltration, where it can have minimal effect on the fabric heat loss of the room as it subsequently degrades. All large areas of insulation are provided either by Styrofoam or glass fibre quilt.

2.3 Airtightness

It is difficult to measure the rate of fresh air ingress into a building as it is subjected to external climate. It was therefore decided that *the* EMC test rooms should be made as airtight as possible to reduce infiltration, and that fresh air would be provided via a mechanical ventilation system which could be easily controlled and metered.

The amount of infiltration into each of the test rooms is governed by the total leakage area in the room

envelope. A range of measures were taken at the construction stage to ensure that the rooms were as airtight as possible:

- the external plywood facing was glued and then nailed to the framing members to make the whole building a stressed skin construction of considerable rigidity. Gluing also prevents infiltration into the wall around the nail holes as the timber swells and shrinks,
- all internal junctions between the plywood facing and timber framing members were sealed with beads of mastic,
- all junctions between adjacent timber panels were sealed with expanding polyurethane foam and/or mastic before fixing the internal finishes in the rooms,
- having nailed the plasterboard to the walls and ceiling the nail heads were driven a few millimetres below the surface and plasterboard filler used to make good. Joints between adjacent sheets of plasterboard were carefully filled with joint filler which was worked into the gaps to the full thickness of the board. The joints were subsequently taped to ensure that, should the joints crack due to movement of the timbers, airtightness would be maintained,
- in the roof space at the top of the side and north walls, expanding polyurethane foam was used to seal the gap between the plywood cladding and the ceiling frame. This prevents air escaping into the unsealed roofspace from the insulation filled wall cavity,
- gaps around the doors and window infill panels were sealed with compressible synthetic rubber gaskets. Pressure on the gaskets is maintained by mechanical fastenings, and finally,
- all holes where cables enter the rooms were sealed with either mastic or hermetic sealing grommets.

After construction the test rooms were pressure tested to determine that they were sufficiently airtight. The pressure testing equipment consisted of a small centrifugal fan and an orifice plate to measure the resulting flow. The orifice plate was constructed and mounted in accordance with the relevant British Standard [5]. Pressure measurements, between the test room and outside and across the orifice plate, were made using a calibrated electronic micromanometer. Sufficiently airtight was defined as a level of infiltration corresponding to less than 1% of the total room energy balance, which was calculated as 0.05 ac/h.

It was realised that the airtightness of the rooms could deteriorate as the rooms were used, due either to gradual degradation of the structure, or to errors when reconfiguring experiments, for example misplaced gaskets around the doors or window frames. It was thus decided that the rooms should be pressure tested each time they were reconfigured, and after being unused for long periods. The time taken to carry out a comprehensive test of the type described above on each of the eight rooms would be prohibitive, and so a simple criterion for a quick test was derived from those results. This criterion was that the rooms should have a leakage rate of less than 1 ac/h at 50 Pascals.

At one stage in the operation of the rooms this pressurisation procedure detected a significant leakage rate in the two test rooms fitted with the oldest window units. Smoke tests carried out whilst the buildings were under pressure revealed a leakage path round the edge of the single glazing, caused by the drying out and associated contraction of the putty in which the glazing contactor had seated the glass. The problem was quickly rectified using a silicone sealant around the edge of the glazing. This example serves to indicate the effectiveness of regular pressure testing as a quality assurance measure, and to indicate the potential dangers of using external contractors who are not familiar with the slightly unusual application of their work.

2.4 Post-operation checks (decommissioning)

When a test room is no longer required for data collection, careful dismantling can serve to ensure that the original construction was as assumed, and that no undetected long term degradation has taken place. Recently, the double glazed EMC test room used in the IEA validation task was inspected in this way by an independent third party, Mr Herbert Eppel of De Montfort University Leicester.

The construction of the entire test room was checked against the working drawings of the room, as reproduced in part 1 of the Validation Package, the Site Handbook. A floorslab was lifted and its thickness measured. A sample of the Styrofoam beneath was cut out and also measured. A small sample was then cut from the chipboard which supports the floor, and that material measured. The floor cavity was inspected through the resulting hole. Figure 2.1 shows the floor being dismantled.

Panels of plasterboard approximately 200 x 200 mm were then cut from the room side and back walls. For the party wall a second hole was cut through the hardboard lining. In all cases it was then possible to check the thickness of the plasterboard, the width of the air gap, the thickness of the insulation and the dimensions of the wall framing members. Figure 2.2 shows the test section cut from the side wall. To check that no insulation was missing small holes were cut through the plasterboard at regular intervals for inspection. Figure 2.3 shows some of these inspection holes in the rear and external side walls of the room.

The construction of the test room front can be examined directly. The construction in the roofspace is also readily accessible, and was thus straightforward to check. Figure 2.4 shows this checking in progress. Measurement of the exposed framing members in the walls of the roofspace (which continue up from the test room walls) provided further confirmation that these were the correct size.

The principal conclusions of the decommissioning exercise were that:

- the test room had been built exactly to the working drawings,
- departures from the nominal timber dimensions were small, typically less than ± 1 mm,
- the thickness of the Styrofoam insulation in the floor was within 0.2 mm of the nominal value of 50 mm,
- the thickness of the Rockwool insulation used in the rooms showed relatively wide variations. The effect was worst in the test room ceiling, where in some places the 100 mm insulation showed variations in thickness as large as ± 20 mm,
- the concrete floorslabs were typically 2 mm thinner than their nominal value of 38 mm,
- the plasterboard lining of the room walls was found to have a thickness of 13.0 mm, compared to the nominal value of 12.7 mm. At least part of this very small discrepancy can be attributed to the paint which has been applied,
- no insulation was missing and all insulation materials were dry,
- there was no evidence of rodent damage. In particular the expanding foam used to seal the tops of the wall cavities in the roofspace, and used to seal between the Styrofoam sheets in the floor was intact,
- the floor cavity beneath the room was still well ventilated, and
- the dimensions of the window were within ± 1 mm of the values specified in the test room

specification. However, there is also a thin bead of silicon around the edge of the glass which further reduces the glazed area. In the case of the double glazed unit the metal spacer also intrudes into the glazed area by up to 3 mm.

Of these findings the variation in the thickness of the installed Rockwool was considered the most serious. In determining the uncertainty in the predicted energy consumption the thickness of the Rockwool has been assumed to be known to within ± 10 mm [3]. However, this variation was assumed to occur across the whole area of the insulation, whereas the variations observed, although larger, occur only in some places. The derived uncertainties are therefore still considered representative.

The discrepancy observed in the thickness of the concrete floorslabs is of less importance. The density quoted for the slabs was determined by weighing a series of slabs and dividing the average mass by the nominal volume. Thus there will be no error when a simulation model calculates the thermal capacity of the floor using this density and the nominal dimensions. An error will occur when the resistance of the slabs is calculated but this will have a limited effect because the slab resistance forms only a small part of the overall resistance of the floor construction.

The small variations in the sizes of the framing timbers will be most significant when calculating the corrections for edge effects. A large uncertainty ($\pm 30\%$) has been associated with the results of those calculations, and this should more than account for the dimensional variations observed.

The small reduction in the effective glazed area of the room has also been accounted for in the determination of the overall uncertainty of predictions of the room performance. The glazed area was assumed to have an uncertainty of ± 0.02 m² associated with it, which adequately allows for the effects noted above.

2.5 Site location

The location of the test rooms was originally obtained by measurement from a 1:50 000 UK Ordnance Survey map [6]. On this basis the site location was quoted as:

Latitude: 52.066° North

Longitude: 0.633° West

A typographical error in the first description of the test facility [1] caused the site longitude to be reported in error as 54.066°N. However the problem was spotted soon after the document was issued, and has been corrected in subsequent versions [2].

Recently (1992) a satellite global positioning system was used to confirm these figures independently. At the time of the test strong signals were received from five satellites. The global positioning system reported the site location as:

Latitude: 52.068° North

Longitude: 0.633° West

The level of agreement between these figures can be fully appreciated by realising that the 0.002° latitude discrepancy represents a distance on the ground of approximately 200 m.

The test site is situated by the side of an airfield, and its altitude is thus well known.

The orientation of the cells was determined by measurements on the shadows cast by the rooms, in conjunction with accurate calculation of solar position.

3 MATERIAL PROPERTIES

Past applications of the data from the test rooms have not made great use of measured material properties. When carrying out component tests or investigation into the physical processes governing the performance of the rooms the overall properties of the rooms are normally included in the analysis as unknowns, which are then determined. When using data from the rooms for model validation book values have been assumed for the materials, as this is the situation under which a simulation modeller would normally operate. Together with the book values estimates of the uncertainties in the properties have been formed, and these have been used to generate the overall uncertainty in the simulation results which are to be compared with results from the rooms. These estimates are the result of combining uncertainties from four sources [3]:

- a) measurement uncertainties in the manufacturers' original tests of their products. For example, if measurements of thermal conductivity are carried out in accordance with the appropriate British Standard [7] an accuracy of $\pm 3\%$ may be assumed for the results,
- b) subsequent variations between batches of the same material,
- c) variations in material properties with age. As discussed above, attempts have been made to minimise these effects by careful choice of material, and
- d) variations of properties with change of operating environment, for example moisture content or working temperature. The magnitude of these effects depends strongly on the type of material and property considered. For some combinations they may be large: for example, the thermal conductivity of insulation materials may vary by as much as 6% for a 10°C change in mean operating temperature.

The effect of obtaining measured values for the materials used in the rooms would be to remove source (b) from this list and, if the measurements were carried out repeatedly, source (c). This would yield a small reduction in the overall uncertainty in the material properties. This would in turn give a small reduction in the uncertainty which could be attributed to simulations of the test room performance. In the past, and in the light of the above discussion, the considerable resource required to test and retest materials in this way has not generally been considered justifiable.

3.1 Insulation materials

The insulation of the test rooms is provided by Styrofoam in the floor, and by a glass fibre quilt in the walls and ceiling. Extensive test data is available from the manufacturers of these materials and this has been used.

3.2 Thermally massive materials

The thermal mass of the rooms is attributable largely to the concrete floorslabs and the plasterboard used to line the walls. Manufacturer's figures have been used for the properties of the plasterboard. However, concrete slabs are produced with a wide range of densities and hence thermal capacities. The density of the floorslabs was determined by weighing them on site, after they had been conditioned in the test rooms.

3.3 Opaque surface properties

The solar reflectance of the white paint used on the interior walls of the test rooms was measured using an integrating sphere spectrophotometer [8]. The reflectance of the sample was measured at 20 wavelengths over the range 0.3 to 2.3 μm . The measured values were then weighted with a solar spectrum and combined to give a total solar reflectance.

3.4 Glazing

The material properties used for the test room glazing have been taken from the glass manufacturer's literature. The thickness of the glass and the size of the air gap in the double glazed units were confirmed by direct measurement at the time of installation.

4 INSTRUMENTATION

The data acquisition system at the test room site automatically records the values of all the quantities measured on site. Depending on the nature of the sensor output this process involves either two or three stages:

- the sensor must convert the physical quantity measured (temperature, radiation, etc) into an electrical output which may be analogue (voltage, current or resistance) or digital (a stream of pulses),
- for the sensors which produce an analogue output the data acquisition system must convert this value into a digital output,
- the data acquisition system must then average or total each of these values over the appropriate time period and record the results on the data disk.

To establish the quality of any given measurement each of these stages must be tested. This may be done by testing the total system: the sensor is subjected to a known excitation and the data disk is checked to see that the correct value has been recorded. When calibration cannot be carried out on site this approach is not feasible, as it would entail shipping not only the relevant sensors but also the whole data acquisition system to the remote calibration laboratory. In this case the sensor must be calibrated alone by the remote laboratory. It is then necessary to establish separately that the remaining two steps in the data acquisition process are being correctly carried out.

4.1 Temperature

Before use, all the temperature sensors used in the test rooms are calibrated against the company reference thermometer. This is a quartz instrument with a resolution of $\pm 0.01^\circ\text{C}$ and a quoted long term drift of less than $0.01^\circ\text{C}/\text{annum}$. The instrument is calibrated every two years by an approved calibration laboratory, giving direct traceability back to UK national standards.

After calibration constants have been derived and fed to the data acquisition system, a process which has been automated to eliminate the risk of human error, a final system check is carried out against the reference thermometer. This serves to check that the entire temperature measuring system is functioning correctly.

4.2 Solar radiation

The primary instruments used for the measurement of solar radiation are Kipp and Zonen thermopile pyranometers. These instruments require temperature compensation, and this is applied in software

using the external air temperature measured in an aspirated enclosure.

The Kipp and Zonen pyranometers are calibrated every two years by the UK Meteorological Office. Since this is a sensor calibration only, it is also necessary to ensure that the analogue to digital conversion applied to the system and the subsequent averaging is accurate. This is done by feeding a known reference voltage to the analogue to digital conversion system which is measured and recorded by the data acquisition system. If the measured value departs from the known value by more than 0.1% an error message is recorded. The value written to disk at the end of the recording interval provides a check that averaging is being correctly carried out.

When an experiment is in progress the Kipp and Zonen units are cleaned, checked for internal moisture, and the associated shadow band is adjusted, every three days. Even with this level of maintenance the Kipp and Zonen units can become inaccurate due to condensation or contamination by birds. To detect such problems a set of pyranometers which use silicon sensors, manufactured by Licor, are mounted alongside all the Kipp and Zonen units. The silicon sensors are less accurate than the Kipp and Zonen pyranometers, but they are much less prone to the short term problems discussed above. Continuous comparison of the readings from the two types of instruments then provides a useful running check on the quality of the solar radiation data gathered.

The shadow ring fitted to the Licor unit is smaller than that used with the Kipp and Zonen pyranometers, and therefore requires more frequent adjustment. If adjustment is neglected the diffuse measurement from the Licor units will become erroneous first, and the resulting discrepancies will reveal the need for adjustment before the principal reading from the Kipp and Zonen is compromised.

4.3 Electrical power

Electrical power is measured using pulse output electricity meters to the appropriate British Standard [9]. This is a sensor specification, and it is therefore necessary to check the accuracy of the remainder of the data acquisition system. Since the sensors produce a digital output there is no analogue to digital conversion stage in the chain. The accuracy of the data acquisition system when it is used to count pulses has been checked by injecting known numbers of pulses at different rates. Periodic comparisons between the recorded energy consumptions and manual readings from the display on each meter provide another check that their output is being correctly recorded.

The accuracy of the power measuring system has also been checked with a dummy load, using a calibrated test meter to determine the mains voltage and current through the load. Agreement was found to be within $\pm 1\%$, well within the value of $\pm 2\%$ which is quoted in the British Standard and which we have assumed when quoting confidence intervals for the measurements.

To obtain the highest quality temperature control in the test rooms, control systems which employ a Proportional+Integral+Derivative control law are used in the test rooms. These units regulate the power supplied to the heater in each room by pulsing the heater on and off. In order to check that this action does not affect the accuracy of the electricity meters a further check was carried out with the dummy load in which the power to the load was pulsed at the rate normally used by the controllers with an accurately known 1:1 mark-space ratio. This was found to affect the accuracy of the meter reading by less than 0.2%.

5 ESTABLISHING MATCHING BETWEEN PAIRS OF TEST ROOMS

A great many of the experiments carried out at the EMC test site have been designed on a side-by-side basis: that is they have consisted of comparisons between test rooms which differ only in the aspect of room construction or operation which is under investigation. As a method of experimental design this approach has a number of advantages. In particular many of the experimental uncertainties are

shared between all the rooms in the trial, and their impact may be reduced as a result.

One of the principal problems with such tests is establishing that adjacent rooms are identical, or matched, when they are identically configured.

In practice there will inevitably be small differences in the performance of adjacent rooms, and there are also uncertainties in the measurement of the performance of the rooms. Therefore it is highly unlikely that the identical performance associated with perfect matching will ever be observed in practice.

In the light of these considerations we have explored two approaches to the problem of matching [10]:

- statistical tests can be applied to the observed room performances allow the presence of systematic differences to be confirmed, or whether the variations in performance are possibly due to random fluctuations, and
- since differences between the rooms are inevitable, all that is important is to establish the likely magnitude of those errors over a period of representative climate, or, preferably, to determine the contribution to the errors from different climatic variables.

The latter approach turns out to be the most powerful. If the contributions to the differences due to individual climatic variables *can* be identified they can be individually statistically tested to determine whether they are significant or could just be due to random fluctuations. Once the significant contributors have been identified there may be the possibility of remedying the causes of the observed mismatches.

A procedure has been developed which allows all of these issues to be addressed during an acceptably short (approximately 10 days) experiment. The way in which the rooms are operated during matching and the tests which can be applied to their resulting performance are described in full in [10].

Establishing matching between test rooms does not conclusively demonstrate that errors have not been made in the initial implementation of the test rooms, as the same mistake may have been made in all cases. Neither does periodic matching confirm that their performance is not changing over time, as degradation may be occurring uniformly across all rooms. However there are potential problems of degradation, control and instrumentation which are very unlikely to occur in all rooms simultaneously, and periodic matching represents a valuable tool for detecting these failures.

REFERENCES

- [1] STUDIES IN PASSIVE SOLAR TEST ROOMS: Description of the Test Room Facility. EMC Report to ETSU. May 1986.
- [2] TEST CELLS 3: Description of the test room facility 1987-88. EMC Report to ETSU. September 1988.
- [3] Detailed Model Comparisons: An empirical validation exercise using SERI-RES. EMC Research Report to ETSU 51197-I. June 1991.

- [4] IEA 21C/12B: Empirical Validation of Detailed Thermal Programs using Test Room Data, Final Report (draft); K. Lomas, H. Eppel, C. Martin, D. Bloomfield; September 1993, IEARN376/93.
- [5] British Standard 1042: Part 1. Methods for the Measurement of Fluid Flow in Pipes. British Standards Institution.
- [6] UK Ordnance Survey Sheet 153: Bedford and Huntingdon. Landranger Series of Great Britain.
- [7] British Standard 874: The measurement of thermal resistance of materials.
- [8] Evaluation of the solar reflectance of four samples of painted cement submitted for test by the Cardiff University Industry Centre. EETS Report no. 2. B M Cross. February 1986.
- [9] British Standard 5685: Electricity Meters. British Standards Institution.
- [10] Matching Trials in the ETSU Test Rooms. EMC Internal Report. October 1988.

FIGURES



Figure 2.1: Dismantling the test room floor

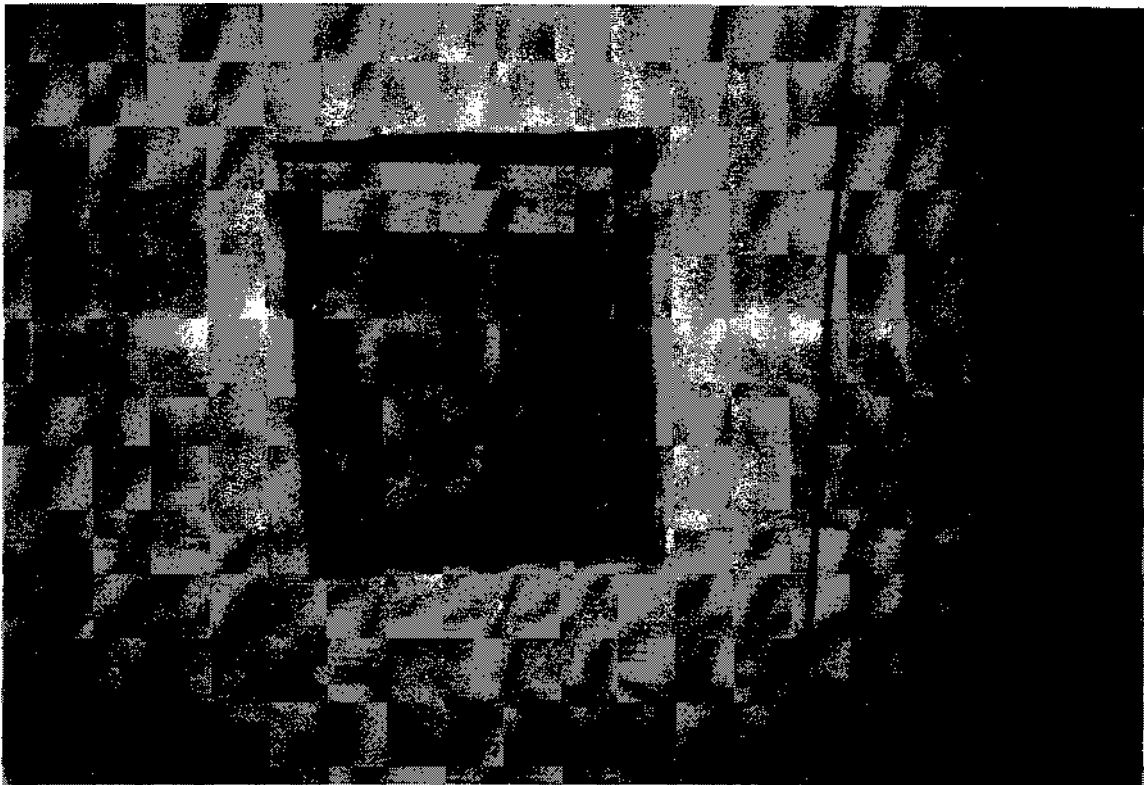


Figure 2.2: Access panel cut from external side wall



Figure 2.3: Inspection holes cut to examine insulation



Figure 2.4: Inspecting the test room ceiling construction

This Data Disk can be used in conjunction with the preceding 3 parts of this document to evaluate the performance of thermal simulation programs of buildings.

The disk contains the two sub-directories 'climate' and 'measured'. Please refer to Part 2 of this document (Validation Guidebook) for guidance on how to use the data.

The contents of the files in the 'climate' directory are described in Section 7 and Appendix 3 of Part 3, the Site Handbook.

The sub-directory with the measured building performance data contains a README file which describes the format.